



Published in final edited form as:

*Eur J Nucl Med Mol Imaging*. 2022 July ; 49(8): 2844–2868. doi:10.1007/s00259-022-05706-y.

## Clinical summary of fibroblast activation protein inhibitor-based radiopharmaceuticals: cancer and beyond

Mengting Li<sup>1,2</sup>,

Muhsin H. Younis<sup>3</sup>,

Yongxue Zhang<sup>1,2</sup>,

Weibo Cai<sup>3</sup>,

Xiaoli Lan<sup>1,2</sup>

<sup>1</sup>Department of Nuclear Medicine, Union Hospital, Tongji Medical College, Huazhong University of Science and Technology, Wuhan, China

<sup>2</sup>Hubei Key Laboratory of Molecular Imaging, Wuhan, China

<sup>3</sup>Departments of Radiology and Medical Physics, University of Wisconsin-Madison, Madison, WI, USA

### Abstract

Fibroblast activation protein (FAP) is a type II membrane-bound glycoprotein which is overexpressed in cancer-associated fibroblasts and activated fibroblasts at wound healing/inflammatory sites. Since the first clinical application of quinoline-based FAP ligands in 2018, FAP inhibitor (FAPI)-based PET imaging and radiotherapy have been investigated for a wide variety of diseases, both cancerous and non-cancerous. As a consequence, promising strides have been made in particular to improve the understanding of FAPI-based PET imaging and the potential value of FAPI-based tumor radiotherapy. Herein, we present a comprehensive review of radiolabeled FAPI, including their clinical translation, in order to clarify the current and potential future role of this class of molecules in nuclear medicine. In particular, this review underlines the value of FAPI radiopharmaceuticals in the diagnosis or therapy of tumors or benign conditions. However, limitations in present studies have hampered a precise evaluation of FAPI radiopharmaceuticals. Despite this, it will likely be worthwhile to further explore the clinical value of FAPI in diagnosis and therapy through better-designed and larger-population clinical trials in the future.

### Keywords

Fibroblast activation protein (FAP); Positron emission tomography (PET); FAP inhibitor (FAPI); Molecular imaging; Cancer; Fibrosis

---

✉ Weibo Cai, [wcai@uwhealth.org](mailto:wcai@uwhealth.org); ✉ Xiaoli Lan, [xiaoli\\_lan@hust.edu.cn](mailto:xiaoli_lan@hust.edu.cn).

**Conflict of interest** Weibo Cai is a scientific advisor, stockholder, and grantee of Focus-X Therapeutics, Inc. All other authors declare no conflict of interest.

**Ethics approval** This article does not contain any studies with human participants or animals performed by any of the authors.

## Introduction

For over 40 years,  $^{18}\text{F}$ -fluorodeoxyglucose (FDG) has been the dominant PET tracer in neurology, cardiology, and, importantly, oncology [1]. As a consequence,  $^{18}\text{F}$ -FDG was once described as “the molecule of the twentieth century.” Combined with the development of PET/CT,  $^{18}\text{F}$ -FDG is now widely used in cancer diagnosis, staging, prognosis, and treatment monitoring. Despite increasing exploitation of more specific tracers in certain malignancies, such as octreotate in neuroendocrine neoplasia [2] and prostate-specific membrane antigen (PSMA) tracers for prostate cancer evaluation [3, 4], the pan-tumor PET agent  $^{18}\text{F}$ -FDG still holds hegemony in oncology. Although data are preliminary, emerging evidence suggests that small-molecule fibroblast activation protein inhibitor (FAPI) tracers may be candidates for widespread oncological application and some benign conditions.

Malignant tumors are composed of neoplastic cells and various non-malignant cells that form and shape the tumor’s microenvironment, or, tumor stroma [5]. Since the stroma can account for 90% of total tumor volume, stroma-targeted imaging may be more sensitive than imaging that targets the tumor cells themselves in some cancers [6]. Cancer-associated fibroblasts (CAFs), a heterogeneous population of fibroblast-like cells, make up most tumor stroma and play a critical role in tumor growth, migration, metastasis, remodeling the extracellular matrix, therapy resistance, and immunosuppression [5, 7]. CAFs are genetically more stable and less susceptible to the development of therapy resistance than cancer cells, therefore being an excellent target cell for antitumor therapy [5-8]. Although the origins of CAFs are heterogeneous, the development of CAFs in tumor stroma is accompanied by morphological changes and the expression of specific surface markers, such as fibroblast activation protein (FAP). According to the current literature, FAP is upregulated in more than 90% of epithelial cancer stroma [9, 10] and some benign conditions such as wound healing, fibrosis, arthritis, and atherosclerotic plaques [11, 12].

FAP is a type II membrane-bound glycoprotein belonging to the dipeptidyl peptidase 4 (DPP4) family with both dipeptidyl peptidase and endopeptidase activity, owning 52% identity at the protein level with DPP4 [13]. The enzyme only transiently expressed during embryonic development, however it may be related to tissue remodeling rather than a necessary component for embryonic development. At present, FAP is not generally nor widely expressed in healthy adults, but there are exceptions. In particular, it is expressed in granulation tissue during wound repair, the cervix, endometrium, pancreas, placenta, and skin [8, 14]. Additionally, soluble FAP was recently found in human plasma, but its origin and function remain unclear [15]. Interestingly, *in vivo* experiments have discovered FAP expression at a basic level in various other tissues, including muscle and bone marrow, which support a hypothesis that FAP may play an important role in maintaining normal muscle function and hematopoiesis. Finally, FAP is expressed in activated fibroblasts but not in resting fibroblasts [13]. These exciting phenomena are the motivation for the use of FAP as a potential target for the diagnosis and treatment of tumors and the diagnosis of non-malignant disease associated with remodeling of the extracellular matrix [8, 16]. Targeting of FAP has been reported using a variety of approaches, including antibodies [17], vaccines [18], immunoconjugates [19], CAR T cells [20], peptide drug complexes [21], and FAP inhibitors (FAPI) [22, 23].

In this review, we will provide an overview focusing on FAP-based radiopharmaceuticals and their clinical application in the diagnosis and therapy of cancers as well as other benign conditions.

## Radiopharmaceuticals based on FAPIs

Meletta et al. have attempted FAP imaging employing a boronic acid-based FAPI molecule, MIP-1232 [24]. In this preclinical study, MIP-1232 was radiolabeled with  $^{125}\text{I}$  as a radiotracer for atherosclerotic plaques and tumors. However, the inhibitor's viability for further application was hampered by the observation that it displayed a similar binding affinity in both plaques and normal arteries, as well as that it permitted limited resolution with gamma imaging. More recently, many quinoline-based FAPI radiotracers have been developed for PET/CT imaging, and various monomeric FAPI analogs were found to have favorable features for use as a radiotracer. In particular, they can be rapidly excreted by the renal system and therefore are quickly cleared from the body, allowing for negligible exposure of healthy tissue to radiation. Additionally, they bind to FAP with very high specificity, are rapidly internalized, and have limited uptake in the brain, liver, and oral-laryngeal mucosa. Researchers have also developed albumin binder-conjugated FAPI radiotracers to prolong blood circulation time. It was demonstrated that after injecting these tracers, uptake in the gallbladder and intestine was high, indicating that they were metabolized and excreted rapidly through the liver, gallbladder, and intestine [25, 26].

In contrast to  $^{18}\text{F}$ -FDG, FAPI-PET may benefit from its independence of blood glucose levels, the fact that it does not require rest beforehand, and quick image acquisition (10 min after tracer application). All of these advantages are clinically practical since they will improve patient comfort and compliance as well as simplify clinical workflow; however, the independence of blood glucose levels means that FAPI-PET is feasible in diabetic patients [7, 8, 27-30]. Regarding the practicality of FAPI-radiotracer production, most FAPI radiotracers studied to date are labeled with  $^{68}\text{Ga}$ , which can be produced in small PET centers without an on-site cyclotron using a  $^{68}\text{Ge}/^{68}\text{Ga}$  generator. On the other hand, the short half-life of  $^{68}\text{Ga}$  and the relatively small activities obtained from a generator may restrict its applications to larger medical centers. Furthermore, the cost of  $^{68}\text{Ge}/^{68}\text{Ga}$  Ga generators as well as the sacrifice of lower resolution for PET imaging of  $^{68}\text{Ga}$  compared to  $^{18}\text{F}$  should also be considered. Thus, the prospect of radiolabeling FAPI with  $^{18}\text{F}$  has recently been investigated in both preclinical and clinical studies [31, 32].  $^{18}\text{F}$ -labeled FAPI was synthesized with a high radioactivity yield as well as radiochemical purity and demonstrated excellent pharmacokinetics and tumor uptake in normal models and tumor patients. Moreover, the universal DOTA-chelator can be attached to FAPI ligands, which may enable theranostics due to their ability to be labeled with an appropriate therapeutic radionuclide [33]. The structure of common FAPI variants labeled with various radionuclides in preclinical or clinical studies is presented in Fig. 1 [34-42].

## Clinical applications of FAP imaging

### FAPI-based imaging of cancer

Clinical evaluation of quinoline-based PET tracers has been done in a spectrum of cancers. Most of these studies were retrospective evaluations, and the patient population was relatively small with different types of cancer. Lately, more data for individual tumors and prospective studies have started to emerge.

### Glioma

Gliomas, the most common primary intracranial tumors, are subdivided into isocitrate dehydrogenase (IDH)–wildtype (wt) gliomas and IDH-mutant (mut) gliomas, according to the World Health Organization (WHO) classification of 2016 [43]. In gliomas, FAP expression has been revealed in spindle-shaped fibroblast-like and perivascular cells, as well as in neoplastic glial cells [44, 45]. These findings make FAPI-PET/CT an attractive tool for imaging of glioma. Röhrich et al. [46] performed  $^{68}\text{Ga}$ -labeled FAPI-02/04 for PET imaging in 18 glioma patients (5 IDH-mutant gliomas, 13 IDH-wildtype glioblastomas). Clear tumor delineation was observed in IDH-wildtype glioblastomas and high-grade IDH-mutant gliomas (III/IV, but not grade II) due to elevated tracer uptake in the tumor site and low background activity in healthy brain parenchyma. This suggests that  $^{68}\text{Ga}$ -FAPI-02/04 may allow a non-invasive distinction between low-grade IDH-mutant and high-grade gliomas (Fig. 2). Another study conducted by the same group revealed that  $^{68}\text{Ga}$ -FAPI-02/04 uptake showed a moderately positive correlation with relative cerebral blood volume (rCBV), whereas no correlation with apparent diffusion coefficient (ADC) was observed [47]. This finding suggests that FAP-specific imaging does not merely reflect tumor cellularity or perfusion, but the spot-like expression of FAP as well. More recently, based on previous studies of a  $^{68}\text{Ga}$  labeled-FAPI monomer, a novel albumin-binding FAP trace  $^{68}\text{Ga}$ -Alb-FAPtp-01 was developed to verify the diagnostic efficacy of imaging glioma. The results demonstrated prominent tumor uptake with improved pharmacokinetics and an increasing SUV and tumor/muscle ratio over time [48]. In light of these results, it is reasonable to suggest that further studies should be designed for assessing the prognostic efficacy of FAPI tracers. Moreover, the use of  $^{68}\text{Ga}$ -FAPI variants compared with conventional PET tracers such as  $^{18}\text{F}$ -FDG,  $^{18}\text{F}$ -fluroethyltyrosine, and  $^{11}\text{C}$ -methionine warrants further study as well.

### Nasopharyngeal carcinoma

Nasopharyngeal carcinoma (NPC) is a malignant epithelial tumor with a significant geographical and ethnic distribution, particularly common in southern China [49]. Regional nodal involvement as well as skull-base and intracranial invasion is frequent in NPC. As with several other types of cancer, mapping the extent of tumor invasion in its early stages is critical for treatment planning and prognosis [50]. In a prospective study [39], 15 patients diagnosed with NPC were enrolled to compare the diagnostic ability of  $^{68}\text{Ga}$ -FAPI-04 and  $^{18}\text{F}$ -FDG PET/MR (Fig. 3). Owing to deficient physiological activity in normal brain tissue and the oropharynx,  $^{68}\text{Ga}$ -FAPI-04 outperformed  $^{18}\text{F}$ -FDG in recognizing the primary tumor and detecting metastases in skull-base and intracranial invasion. Based on the favorable soft-tissue resolution in MRI, Qin et al. suggested that  $^{68}\text{Ga}$ -FAPI-04 hybrid

PET/MR may potentially serve as a single-step imaging modality for patients with NPC. Another retrospective analysis was conducted by Zhao et al., who enrolled 45 participants to explore the clinical utility of  $^{68}\text{Ga}$ -FAPI-04 PET/CT relative to  $^{18}\text{F}$ -FDG PET/CT and MRI for primary staging and recurrence detection in NPC [40]. In initial assessment patients,  $^{68}\text{Ga}$ -FAPI-04 PET/CT showed higher uptake in primary tumors, regional lymph nodes, and bone and visceral metastases than  $^{18}\text{F}$ -FDG. Also,  $^{68}\text{Ga}$ -FAPI suggested an advanced stage of cancer, evaluated by the TNM staging system, in ten patients, which resulted in a management change in seven of these patients. For post-treatment patients,  $^{68}\text{Ga}$ -FAPI-04 yielded more true-positive findings than  $^{18}\text{F}$ -FDG in detecting local recurrence. Compared with MRI,  $^{68}\text{Ga}$ -FAPI-04 PET/CT detected upgraded cancer stages and underestimated the T stage in four and two patients. The authors therefore suggest that  $^{68}\text{Ga}$ -FAPI-04 PET/CT may be supplementary to MRI for T staging and radiotherapy planning. Similarly, Shang et al. reported a case in which a detection of metastases in the cervical lymph nodes by  $^{18}\text{F}$ -FDG-PET/CT was found to be a false-positive, and subsequently found to have no abnormal  $^{68}\text{Ga}$ -FAPI uptake visible with FAPI-PET/CT (it was unclear which specific FAPI-based tracer was used in this study, likely  $^{68}\text{Ga}$ -FAPI-04). Unfortunately, the patient received unnecessary chemotherapy. In this case, and perhaps more generally,  $^{68}\text{Ga}$ -FAPI-PET/CT might have been useful for assessing pretreatment lymph node status in NPC and avoiding an unnecessary treatment [51]. In some cases, it can be challenging for  $^{18}\text{F}$ -FDG to diagnose head and neck cancer of an unknown primary tumor. Gu et al. carried out a study in which eighteen patients with negative  $^{18}\text{F}$ -FDG findings were enrolled.  $^{68}\text{Ga}$ -FAPI-04 PET/CT detected the primary tumor in 7 out of 18 patients, and subsequent biopsies and histopathological examinations were then performed to verify these findings. This pilot study presented evidence to improve the detection rate and diagnostic role of  $^{68}\text{Ga}$ -FAPI-04 PET/CT in head and neck cancer of unknown primary tumor patients with negative  $^{18}\text{F}$ -FDG findings [52]. Although these clinical trials exhibit promising results, several limitations of these studies cannot be ignored. The sample sizes were generally relatively small, and not all positive findings were confirmed histopathologically. As such, in order to determine whether  $^{68}\text{Ga}$ -FAPI PET/CT is truly as powerful as these results have indicated, further, well-designed prospective studies are needed.

### Gastric cancer and colorectal cancer

Gastric cancer and colorectal cancer are two common types of gastrointestinal cancer [53]. While  $^{18}\text{F}$ -FDG-PET/CT is valuable in imaging gastrointestinal malignancies, some limitations must be noted, in particular low sensitivity in detecting primary lesions, liver metastases, and peritoneal carcinomatosis [54]. On the other hand, in a mixed cancer population study, Pang et al. [29] demonstrated the superior value of  $^{68}\text{Ga}$ -FAPI-04 PET/CT over  $^{18}\text{F}$ -FDG in detecting primary and metastatic lesions in gastric and colorectal cancers, with most lesions showing higher tracer uptake with FAPI imaging. In another study, Zhao et al. observed that  $^{68}\text{Ga}$ -FAPI-04 PET/CT outperformed  $^{18}\text{F}$ -FDG in detecting peritoneal carcinomatosis, particularly in patients with gastric cancer (Fig. 4) [55, 56]; these results are in line with those of another group, Kuten et al. [57]. Furthermore, in the study by Kuten et al., two patients with peritoneal carcinomatosis underwent a follow-up  $^{68}\text{Ga}$ -FAPI-04 PET/CT scan after neoadjuvant chemotherapy [57]. One patient showed disease progression after four months of chemotherapy that manifested as new implants, more diffuse peritoneal

fat infiltration, and a slightly increased average  $SUV_{max}$ , confirming the true-positive results of the initial FAPI-PET/CT scan. After five months of treatment, the other patient had partial remission, with most lesions undetected, abnormal tracer accumulation, and only mild FAPI uptake identified in a few residual implants. Nevertheless, although  $^{68}Ga$ -FAPI PET/CT has shown promise in monitoring response to treatment in patients with peritoneal carcinomatosis, more extensive population trials are needed to validate these preliminary findings.

In a bicentric retrospective analysis with heterogeneous gastric cancer (including adenocarcinoma and signet ring cell carcinoma) by Jiang et al.,  $^{68}Ga$ -FAPI-04 PET showed a superior detection rate over  $^{18}F$ -FDG for primary gastric cancer [58]. In particular, it exhibited better performance in gastric cancer diagnosis and staging. Furthermore,  $^{68}Ga$ -FAPI-04 displayed focal uptake in the primary tumor, whereas  $^{18}F$ -FDG showed slightly and diffusely elevated uptake in the gastric wall. As a result,  $^{68}Ga$ -FAPI-04 apparently could provide better information when making surgical decisions regarding gastric cancer. Notably,  $^{18}F$ -FDG showed lower sensitivity for the detection of signet ring cell carcinoma; in this study,  $^{68}Ga$ -FAPI-04 outperformed in detecting 3 cases of signet ring cell carcinoma that were not detected by  $^{18}F$ -FDG, resulting in a sensitivity of 100% (7/7) vs. 57% (4/7). Therefore,  $^{68}Ga$ -FAPI-04 PET has an obvious advantage for the detection of signet ring cell carcinoma. However, the sensitivity of  $^{68}Ga$ -FAPI for detecting signet ring cell carcinoma needs to be evaluated in a trial with a larger sample size than those that have been conducted. On another note, tumor size is an important factor influencing the SUV and the detection rate of gastric cancer on PET scans. The authors observed that for detecting tumors less than 4 cm,  $^{68}Ga$ -FAPI-04 PET demonstrated higher sensitivity than  $^{18}F$ -FDG. Although the difference was not significant (100 vs. 71%,  $P=0.062$ ), further confirmation of whether  $^{68}Ga$ -FAPI-04 PET has advantages for the detection of small gastric cancers is needed. The above finding is similar to Qin et al. and could improve diagnostic accuracy, consequently reducing the possibility of missed diagnoses [59].

$^{68}Ga$ -FAPI PET/CT exhibited a promising role in diagnosis, (re)-staging, and radiotherapy planning for lower gastrointestinal cancers. Koerber et al. [60] evaluated the clinical use of  $^{68}Ga$ -FAPI-04 PET/CT in a cohort of 22 patients with malignancies of the lower gastrointestinal tract. The average  $SUV_{max}$  of  $^{68}Ga$ -FAPI-04 in colorectal cancers was intermediate grade ( $SUV_{max}$  of 8.6), consistent with the results of Kratochwil et al. [33]. In half of the treatment-naïve patients enrolled, the TNM staging evaluation was changed, while in 47% of them, new metastatic lesions were recognized. Furthermore, target volume delineation was improved by  $^{68}Ga$ -FAPI-04 PET/CT in patients undergoing irradiation, thus making  $^{68}Ga$ -FAPI-04 PET/CT a promising imaging modality for the diagnosis, management, and treatment planning of colorectal cancers.

### Hepatic carcinoma

Hepatocellular carcinoma (HCC) and intrahepatic cholangiocarcinoma (ICC) are the two most common types of primary hepatic carcinoma. HCC is mainly developed in fibrotic or cirrhotic livers, whereas ICC is a stroma-rich tumor with CAFs several folds more prominent in number than the actual tumor cells [61, 62]. Shi et al. [63] prospectively enrolled 17



patients who had hepatic lesions that were anticipated to become malignant according to CT, MR, and ultrasound. All participants underwent surgery or biopsy for the final analysis. One patient presented benign hepatic nodules with granulation tissue that showed negligible  $^{68}\text{Ga}$ -FAPI-04 uptake. Elevated uptake and target-to-background ratio (TBR) were detected in 16 patients with malignant hepatic lesions, 11 of which were HCC (Fig. 5), 2 were ICC, and 3 were metastatic malignant lesions (from gastric adenocarcinoma, breast cancer, and sigmoid colon adenocarcinoma). These conclusions were also corroborated by a single-center post hoc retrospective analysis conducted by Guo et al. [64]. This study indicated that the sensitivity of  $^{68}\text{Ga}$ -FAPI-04 PET/CT to identify primary liver tumors correctly and metastatic lesions is equivalent to that of CE-CT and liver MRI, while it is better at identifying liver lesions than  $^{18}\text{F}$ -FDG. Furthermore, Wang et al. observed that  $^{68}\text{Ga}$ -FAPI-04 PET/CT showed a higher sensitivity than  $^{18}\text{F}$ -FDG PET/CT in detecting small HCC lesions ( $< 2$  cm in diameter, 68.8 vs. 18.8%,  $P = 0.008$ ) [65]. When comparing among different histologies, higher  $^{68}\text{Ga}$ -FAPI-04 uptake and TBR was noted in ICC (average  $\text{SUV}_{\text{max}}$ ,  $13.55 \pm 2.34$ ; TBR,  $26.92 \pm 4.68$ ) as compared with HCC (average  $\text{SUV}_{\text{max}}$ ,  $7.78 \pm 3.84$ ; TBR,  $9.78 \pm 6.97$ ) and metastases (average  $\text{SUV}_{\text{max}}$ ,  $7.67 \pm 4.56$ ; TBR,  $17.87 \pm 10.61$ ). This finding is consistent with other findings [66], thus suggesting  $^{68}\text{Ga}$ -FAPI-04 as a potential candidate differentiating HCC and ICC. However, there was no significant difference among poorly, moderate, and well-differentiated HCC in  $\text{SUV}_{\text{max}}$  and TBR, indicating difficulties in tumor grading by  $^{68}\text{Ga}$ -FAPI-04. Another notable finding was that hepatic uptake of  $^{68}\text{Ga}$ -FAPI-04 was elevated in patients with cirrhosis and hepatitis. Pang et al. [67] demonstrated that  $^{68}\text{Ga}$ -FAPI showed superior ability to detect primary tumors and reveal more metastatic lesions, especially bone micro-metastases, than  $^{18}\text{F}$ -FDG in an ICC patient (it was unclear which specific FAPI-based tracer was used in this study, likely  $^{68}\text{Ga}$ -FAPI-04). Additionally, Zhao et al. have reported a case in which MRI falsely characterized benign nodules as HCC, while  $^{68}\text{Ga}$ -FAPI correctly characterized them, further demonstrating the value of  $^{68}\text{Ga}$ -FAPI in HCC diagnosis (it was unclear which specific FAPI-based tracer was used in this study, likely  $^{68}\text{Ga}$ -FAPI-04) [68].

### Pancreatic cancer

Pancreatic cancer is a lethal malignant cancer, with a 5-year survival rate of  $< 10\%$ . Still, early detection and diagnosis of cancer are crucial for prolonging patient survival [53]. Since  $^{18}\text{F}$ -FDG PET/CT has limited sensitivity for detecting lymph nodes, liver metastases, and peritoneal carcinomatosis, the National Comprehensive Cancer Network (NCCN) guidelines do not recommend  $^{18}\text{F}$ -FDG PET/CT as the first-line imaging modality for the diagnosis of pancreatic cancer [69, 70]. Pang et al. retrospectively analyzed the detection and staging ability of  $^{68}\text{Ga}$ -FAPI-04 compared to  $^{18}\text{F}$ -FDG-PET/CT in 26 patients with suspected or diagnosed pancreatic malignancy [71]. The results demonstrated that  $^{68}\text{Ga}$ -FAPI-04 outperformed  $^{18}\text{F}$ -FDG in tumor radiotracer uptake and detection rate of primary tumors, lymph nodes, liver, bone metastases, and peritoneal carcinomatosis (Fig. 6a). Compared with  $^{18}\text{F}$ -FDG and contrast-enhanced CT,  $^{68}\text{Ga}$ -FAPI-04 PET/CT raised the stage of six patients' and five patients' TNM staging, subsequently changing the clinical management in only two patients and one patient, respectively. Furthermore, almost half of patients showed intense  $^{68}\text{Ga}$ -FAPI-04 uptake throughout the pancreas. It is challenging to distinguish pancreatitis from pancreatic cancer via visual interpretation or semiquantitative analysis

at the routine acquisition time of 1 h. The delayed PET/CT scan at three hours showed a decrease in  $^{68}\text{Ga}$ -FAPI-04 uptake within pancreatitis and could therefore play a role in differentiating pancreatitis from malignancy (Fig. 6b). Although  $^{68}\text{Ga}$ -FAPI-04 has shown higher sensitivity in detecting primary pancreatic tumors and metastases while also providing more accurate TNM staging, prospective trials with a larger patient population are once again needed to evaluate whether  $^{68}\text{Ga}$ -FAPI PET/CT could improve treatment planning compared with the standard imaging modality.

Zhang et al. observed that focal  $^{68}\text{Ga}$ -FAPI-04 uptake in the pancreas could happen in some non-malignant diseases, including pancreatic pseudocysts, sites of prior pancreatitis, and foci of immunoglobulin G4-related disease (Fig. 6c). However, the integrative  $^{68}\text{Ga}$ -FAPI-04 PET/MR may potentially decrease the misdiagnosis of some pancreatic lesions [72]. Recently, studies have found that  $^{68}\text{Ga}$ -FAPI-PET/CT could detect multiple foci in pancreatic neuroendocrine tumors, involved lymph node metastases, and liver metastases with increased activities and good tumor-to-liver ratios. Although this phenomenon has only been reported in two cases, it suggests that FAPI-based radiotracers may be helpful in the evaluation and targeted therapy of neuroendocrine tumors [73, 74].

### Other cancer types

Several retrospective studies have found that  $^{68}\text{Ga}$ -FAPI-04/46 PET imaging is superior to  $^{18}\text{F}$ -FDG in detecting primary breast malignancies, lymph nodes, liver metastases, bone metastases, and peritoneal carcinomatosis with high sensitivity, high uptake values, and high TBR (Fig. 7a). Unlike  $^{18}\text{F}$ -FDG, uptake of  $^{68}\text{Ga}$ -FAPI-04/46 appeared to be statistically insignificant with different breast phenotypes [75, 76]. Also, in some cases,  $^{68}\text{Ga}$ -FAPI could supplement finding primary breast lesions and regional lymph nodes that were not well seen or missed by MRI, indicating the potential value of  $^{68}\text{Ga}$ -FAPI tracers for breast cancer diagnosis and staging [76-80]. Although the results were encouraging,  $^{68}\text{Ga}$ -FAPI images led to false-positive and false-negative diagnoses of lymphoid tissue, hepatic lesion, and bone metastasis in a minority of cases [76, 81, 82]. These cases demonstrate that not all FAPI accumulation can be immediately interpreted as malignancy. Likewise, not all lesions with baseline FAPI uptake can be considered normal; in this study, some lesions identified with FAPI-PET had to be confirmed with biopsy or clinical follow up. Still, this study also had its limitations, one of which that it was designed as a retrospective study rather than a prospective one. Also, the cohort of patients may have had a bias toward larger (> 2 cm) or locally advanced disease, which is not an accurate way to estimate sensitivity and specificity in the early stages of progression [75]. Furthermore, the breast is a hormone-sensitive organ, and the FAPI uptake seems to be influenced by hormone levels among other internal factors. Specifically, the presence or absence of the menstrual cycle may be essential for the precise and accurate interpretation of  $^{68}\text{Ga}$ -FAPI PET/CT scans [83, 84].

One retrospective study enrolled patients with mixed tumor entities and histopathologically proven prostate cancer for measurement of  $^{68}\text{Ga}$ -FAPI-04 uptake with  $^{68}\text{Ga}$ -FAPI PET/CT. Intermediate to high  $^{68}\text{Ga}$ -FAPI-04 uptake (the average  $\text{SUV}_{\text{max}}$  6–12) was observed in the primary tumor site and metastases [33]. However, this pilot study only included patients with PSMA-negative tumors, which may cause the selection bias. Moreover, this population only



constituted a minority of prostate cancers; future studies need to be thoroughly investigated in typical prostate cancer patients. Nevertheless, this finding may benefit our understanding of insufficient PSMA expression in PSMA-negative tumors and thereby provide a diagnosis method with radioligand treatment [85]. Regarding other types of prostate cancer, recently Kesch et al. observed that  $^{68}\text{Ga}$ -FAPI-04 PET/CT was highly positive in castration-resistant prostate cancer (CRPC) patients and bone/lymph node metastasis (Fig. 7b). Furthermore, tissue microarray construction and immunohistochemistry showed a significant rise in FAP expression with the advancement of disease from benign tissue to CRPC. The variation in FAP tissue expression supports further investigation of FAPI-radionuclide theranostics in CRPC [86].

Some small mixed population studies demonstrated that differentiated thyroid cancers have low to moderate  $^{68}\text{Ga}$ -FAPI-04 uptake with average  $\text{SUV}_{\text{max}} < 6$ , and that  $^{68}\text{Ga}$ -FAPI-04 outperformed  $^{18}\text{F}$ -FDG in detecting bone metastases [33, 87, 88]. However,  $^{68}\text{Ga}$ -FAPI-04 PET/CT detected more false-positive bone lesions than  $^{18}\text{F}$ -FDG, reducing the overall specificity of this modality. Hence, it is critical to carefully interpret all CT findings to ensure diagnostic accuracy. The diagnosis and treatment of differentiated thyroid cancer with thyroglobulin elevation and negative iodine scintigraphy (TENIS) syndrome or radioiodine-refractory differentiated thyroid cancer (RAIR-DTC) are currently major issues. While  $^{18}\text{F}$ -FDG PET/CT is a common imaging modality for detecting tumor recurrence and metastases, its sensitivity has been found to be insufficient [89, 90]. In recent cases,  $^{68}\text{Ga}$ -FAPI showed a higher signal-to-noise ratio and sensitivity than  $^{18}\text{F}$ -FDG for detecting lesions in small pulmonary metastases as well as liver/bone metastases (Fig. 7c) [91-93]. These findings demonstrate its usefulness in patients with TENIS or RAIR-DTC for localizing recurrent or metastatic lesions. They also highlight the potential for radionuclide-targeted therapy, which may become a cornerstone of therapy for this kind of cancer.

Different degrees of physiological myocardial uptake are common with  $^{18}\text{F}$ -FDG PET and may hamper the detection of cardiac tumors. Conversely, Zhao et al. found a focus with intense  $^{68}\text{Ga}$ -FAPI uptake with a target/myocardium ratio of 3.9 in the right chest in a patient with massive bloody pericardial effusion (it was unclear which specific FAPI-based tracer was used in this study, likely  $^{68}\text{Ga}$ -FAPI-04). Meanwhile, no abnormal activity was observed in this patient by  $^{18}\text{F}$ -FDG. Follow-up with  $^{68}\text{Ga}$ -FAPI PET/MR confirmed increased uptake in the right atrium corresponding to the sites of abnormal MRI signal intensity, and subsequently angiosarcoma was confirmed by histopathological examination (Fig. 7d) [94]. This case indicated that  $^{68}\text{Ga}$ -FAPI is superior to  $^{18}\text{F}$ -FDG in identifying cardiac angiosarcoma, with higher tumor-to-background contrast. In addition to this,  $^{68}\text{Ga}$ -FAPI variants presented uptake in esophageal, pheochromocytoma, renal cell, and diffuse large B cell lymphoma, which may indicate more new applications in multiple tumor types for noninvasive detecting, staging, or radioligand therapy [33, 95, 96].

## FAPI-based imaging of non-cancerous diseases

### Immunoglobulin G4-related disease

Immunoglobulin G4-related disease (IgG4-RD) affects multiple organs with histopathological characterization by “storiform” fibrosis. Luo et al. investigated the

performance of  $^{68}\text{Ga}$ -FAPI-04 in imaging IgG4-RD (Fig. 8) [97]. This prospective cohort study showed that  $^{68}\text{Ga}$ -FAPI-04 was superior or equal to  $^{18}\text{F}$ -FDG for detecting IgG4-RD in the lacrimal gland, salivary gland, pancreas, and bile duct/liver in all 26 recruited patients, and more involved sites were capable of being recognized with imaging than only based on symptoms. Similar results were also observed in recurrent IgG4-RD and IgG4-related sclerosing cholangitis by other research groups [98-101]. In contrast, lymph node involvement was FAPI-negative. Further studies to explore the exact mechanism are needed. Recently, Schmidkonz et al. demonstrated the ability of FAPI-PET to non-invasively discriminate inflammatory from fibrotic activity in IgG4-RD [102]. This may provide new insights and profoundly change the management of certain forms of immune-mediated disease.

### Cardiovascular disease

Several systematical research studies have investigated the fibroblast activity caused by myocardial infarction (MI) or cancers in cardiac injury patients using  $^{68}\text{Ga}$ -FAPI PET. A cohort of 10 patients underwent  $^{68}\text{Ga}$ -FAPI-46 PET imaging at an average of 18 days after acute MI (five ST-segment elevation MI and five non-ST-segment elevation MI) [103]. All patients exhibited focal FAPI uptake, while fibroblast activation volume showed an inverse correlation with left ventricular function. A partial to complete match of affected myocardium between tracer uptake was observed, and subsequently confirmed by coronary angiography (Fig. 9a). Another study reported that  $^{68}\text{Ga}$ -FAPI-04 overestimates the infarct size as confirmed by cardiac-MRI [104]. An analysis found a correlation between coronary artery diseases, age, and the left ventricular ejection fraction with FAPI accumulation [105]. Additionally, in a study of 229 patients with metastatic disease, high signal intensities of FAPI uptake were observed associated with cardiovascular risk factors and metabolic diseases [106]. These findings suggest that  $^{68}\text{Ga}$ -FAPI PET/CT may provide a new insight to the investigation of cardiac FAP and the mechanisms of structural/fibrotic remodeling after AMI pathophysiology. Focal or diffuse uptake of  $^{68}\text{Ga}$ -FAPI was found in many other cardiac diseases, including idiopathic or chronic thromboembolic pulmonary arterial hypertension [107, 108], hypertensive heart disease [109], chemotherapy-induced myocardial injuries (Fig. 9b) [110], and status after radiofrequency ablation [111], indicating that  $^{68}\text{Ga}$ -FAPI PET may be a promising modality for imaging cardiac diseases. Another cardiovascular disease for which  $^{68}\text{Ga}$ -FAPI PET may be useful is immune checkpoint inhibitor (ICI)-associated myocarditis, which has a low incidence (around 1.4%) but a high fatality rate (up to 50%) [112]. ICIs are clinically useful in the treatment of cancer, and as such their use is increasing, but they are also known to cause cardiovascular side effects such as ICI-associated myocarditis. In a cohort study,  $^{68}\text{Ga}$ -FAPI PET/CT was used for 26 cancer patients receiving ICIs (it was unclear which specific FAPI-based tracer was used in this study, likely  $^{68}\text{Ga}$ -FAPI-04). Three patients with clinical manifestations of ICI-myocarditis showed elevated median SUVs in the myocardium compared to 23 non-myocarditis patients (Fig. 9c) [113]. This result indicated that  $^{68}\text{Ga}$ -FAPI PET/CT could be a non-invasive method to diagnose ICI-associated myocarditis at an early stage. Moreover, combined with biomarkers, ECG, and echocardiography, it also contributes to cardiac risk stratification. Due to the relatively small number of enrolled patients, further studies need to be carried out

in a larger population to address the predictive value and the best time window to diagnose ICI-associated myocarditis via FAPI-PET/CT.

### Osteoarticular disease

FAP can be found in arthritis and fibrosis [114]. A patient with a history of chronic prostatitis and left shoulder osteoarthritis underwent  $^{68}\text{Ga}$ -FAPI-04 imaging and was found to have abnormal tracer uptake in the prostate (a biopsy confirmed prostate cancer) and the left shoulder [115]. Interestingly, the site of the shoulder arthritis showed higher  $^{68}\text{Ga}$ -FAPI-04 uptake than the tumor site, indicating that  $^{68}\text{Ga}$ -FAPI-04 imaging may not be more tumor-specific than  $^{18}\text{F}$ -FDG. Recently, an increasing number of case studies reported that focal or widespread FAPI uptake could be observed in nonmalignant osteoarthritis, including degenerative osteophyte [87, 116, 117], Schmorl node [87, 118], fracture [119, 120], benign bone cyst [121], fibrous dysplasia [122, 123], ankylosing spondylitis [124], Bastrup disease [125], and osteoarthritis [126]. Although this phenomenon indicates the potential value of  $^{68}\text{Ga}$ -FAPI imaging in inflammation, it may hamper its usefulness in tumors. Since patients undergoing FAPI imaging usually have a history of cancer, the false-positive of  $^{68}\text{Ga}$ -FAPI uptake in some benign bone lesions suggests that radiologists should consider all clinical data comprehensively in the diagnosis.

### Other diseases

Zhou et al. [127] indicated that  $^{68}\text{Ga}$ -FAPI PET/CT might be useful in imaging thyroiditis and identifying benign/malignant thyroid lesions (it was unclear which specific FAPI-based tracer was used in this study, likely  $^{68}\text{Ga}$ -FAPI-04). Gu et al. [128] reported a case with extrapulmonary tuberculosis mimicking a malignant tumor showing intense  $^{68}\text{Ga}$ -FAPI uptake (it was unclear which specific FAPI-based tracer was used in this study, likely  $^{68}\text{Ga}$ -FAPI-04). This finding was similar to Hao's report, which demonstrated that  $^{68}\text{Ga}$ -FAPI-04 PET/CT showed higher uptake in lung, spine, and brain tuberculous lesions and may help delineate the lesion extent in disseminated infection [129]. An increasing number of clinicians have observed increased uptake of  $^{68}\text{Ga}$ -FAPI in wound healing, pancreatitis, Erdheim-Chester disease, Crohn's disease, and so on, demonstrating its capability as a nonspecific tumor agent [130-133]. These observations demonstrate the potential of  $^{68}\text{Ga}$ -FAPI to image inflammation, which is important for clinicians to keep in mind when interpreting  $^{68}\text{Ga}$ -FAPI images of patients with either cancer or inflammation, lest they ignore the other.

### Radiotherapy planning with FAP imaging

Radiation therapy (RT) is one of the essential modalities of treatment for various types of cancers. The definition of the target volume to precision differentiation of tumor and adjacent healthy tissue is directly relevant to tumor therapeutic effect and toxicity to healthy tissue, making imaging an essential aspect of RT planning.

Syed et al. [134, 135] analyzed FAPI-based gross tumor volume (FAPI-GTV) using four different TBR thresholds (three-, five-, seven-, and tenfold) with conventional (CT-GTV) on 14 patients with head and neck cancers. Ah FAPI-GTVs were significantly different

from conventional CT-GTVs. Considering an available clinical and imaging information, three times FAPI threshold (FAPI  $\times$  3-GTV, medium 66.7 ml, range 6.0–292.7) seemed to be reasonable for delineating tumor and healthy tissue in clinical practice. Windisch et al. [136] compared FAPI-GTV with MRI-GTV in 13 wild-type IDH glioblastoma patients. The result from MRI-GTVs was statistically smaller than FAPI  $\times$  5-GTV but equal to and larger than FAPI  $\times$  7 and FAPI  $\times$  10, respectively. Furthermore, adding FAPI-GTVs to MRI-GTVs significantly increased the GTV for all three thresholds. Röhrich et al. compared the value of  $^{68}\text{Ga}$ -FAPI-02/46/74 PET/CT to conventional contrast-enhanced CT and magnetic resonance imaging for staging and RT planning in adenoid cystic carcinoma patients [137].  $^{68}\text{Ga}$ -FAPI-GTVs were acquired at three time points (10 min, 1 h, 3 h) based on the threshold values of 25–35% of  $\text{SUV}_{\text{max}}$ . Although the median volumes showed insignificant differences, images at 1 h were considered ideal for contouring since there was a considerable amount of non-specific FAPI uptake after 10 min and excessive washout in tumor lesions at 3 h. In several cases, small branches of tumors spreading along nerves, around cranial bones, or through cranial foramina were encompassed in FAPI-GTV but not in CT-GTV. Outstandingly,  $^{68}\text{Ga}$ -FAPI-PET improved the accuracy of actual tumor volume delineation for RT compared to CT and MRI.

Ristau et al. [138] measured the potential usefulness of FAPI-PET/CT in RT planning of esophageal cancer patients. The extraordinary TBR resulted in precise target volume delineation, and FAPI-GTV was perfectly matched with endo-esophageal clipping, the gold standard to define tumor margins. Besides the excellent SUV values in primary esophageal tumors, the excellent ability to detect lymph node metastases using FAPI-PET/CT might provide additional information for target volume planning and help avoid tumor geographic misses [139]. Other research teams also demonstrated the practical value of FAPI-PET/CT on target volume definition in locally recurrent pancreatic cancer, lung cancer, and lower gastrointestinal tract cancer patients [42, 60, 138, 140]. In conclusion, FAP-specific PET represents a promising imaging modality for RT planning that warrants further investigation. Future studies should focus on increasing the patient number and statistical reliability, and decrease the variability of delineation of tumor volumes.

## Cancer treatment with radiolabeled FAPIs

Radionuclide theranostics and personalized medicine work well with one another via the optimum selection of an appropriate radiolabelled probe for the specific patient and form of cancer. In studies employing FAPI-based radiopharmaceuticals, low background in normal tissues with excellent TBR has been observed, making these a possible candidate for tumor theranostics. The macrocyclic bifunctional DOTA chelator enables FAPI to be radiolabelled with  $^{68}\text{Ga}$  in addition to a therapeutic isotope such as  $^{177}\text{Lu}/^{90}\text{Y}/^{225}\text{Ac}$ , making these probes applicable to both PET imaging and radionuclide therapy. Additionally, Lindner et al. [35] conducted the first therapeutic application of  $^{90}\text{Y}$ -FAPI-04 in a patient with metastatic breast cancer (Fig. 10). A dose of 2.9 GBq of  $^{90}\text{Y}$ -FAPI-04 was administered, and persistent localization was confirmed with bremsstrahlung imaging at even 1 day after injection. Furthermore, significant pain palliation was achieved even at the low dose administration, and no systematic side effects were observed.

Although  $^{68}\text{Ga}$ -labeled FAPIs compounds possess a very high rate of internalization of the tumor, a significant efflux resulting in relatively short intertumoral half-lives is still troubling. Developing newer compounds with prolonged tumor retention might be suitable approaches to improve the therapeutic effect. Nowadays, butyric acid-conjugated, truncated evans blue-conjugated, fatty acid-conjugated, and dimer strategies have been developed. These strategies prolonged the blood circulation or enhanced the tumor local FAPI concentration and optimized the pharmacokinetics when compared to their monomeric analogs [25, 26, 48, 140].

Recently, Ballal et al. [142] reported a case of advanced-stage breast cancer treated with  $^{177}\text{Lu}$ -DOTA.SA.FAPI after exhausting multiple lines of chemotherapy. Dosimetry revealed an approximate absorbed tumor dose of 1.48E mGy/MBq and 3.46 mGy/MBq of  $^{177}\text{Lu}$ -DOTA.SA.FAPI to the primary tumor and the brain metastasis, respectively. The patient experienced immediate relief in pain and improvement in quality of life. The authors then explored the safety and effectiveness of this treatment with FAPI-based targeted theranostics as a salvage treatment option in radioiodine-refractory differentiated thyroid cancer [143]. Preliminary data suggested that treatment with dimer  $^{177}\text{Lu}$ -DOTAGA. (SA.FAPI)<sub>2</sub> is safe and effective as a new method to treat aggressive radioiodine-refractory differentiated thyroid cancer patients who have exhausted all standard lines of treatments.

Watabe et al. [37] demonstrated that  $^{225}\text{Ac}$ -FAPI-04 injection exhibited significant tumor growth suppression in PANC-1 xenograft mice in a preclinical study. Furthermore,  $^{64}\text{Cu}$ -FAPI-04 PET/CT showed significantly higher accumulation levels in the tumor and healthy organs than  $^{68}\text{Ga}$ -FAPI-04, suggesting that the  $^{64}\text{Cu}/^{67}\text{Cu}$  theranostic pair could exhibit an exciting effect [1]. Beyond PET imaging, which can be difficult for small medical centers or lower-cost conditions,  $^{99\text{m}}\text{Tc}$ -labeled SPECT may be an alternative to PET. Furthermore, the chemically homologous nuclide  $^{188}\text{Re}$  is available from generators, which may allow FAP-targeted radionuclide therapy [144].

Since FAPIs clear from the tumor more rapidly than other molecules such as PSMA or somatostatin receptor ligands, radionuclides with relatively short half-lives are preferable in order to match the probe's pharmacokinetics.  $^{188}\text{Re}$ ,  $^{153}\text{Sm}$ ,  $^{213}\text{Bi}$ , or  $^{212}\text{Pb}$  may be much more suitable and deliver higher doses to tumor sites [7, 144]. Recently, a patient with lung metastases of a sarcoma underwent  $^{153}\text{Sm}$ -labeled FAPI-46 radionuclide therapy [145]. The short physical half-life (46.3 h) of  $^{153}\text{Sm}$  is a good match for the relatively short biological half-life of FAPI-46. Emission scans during therapy demonstrate tumor targeting up to 44 h p.i. and rapid clearance from normal organs. The patient achieved stability for eight months after three treatment cycles with a cumulative 20 GBq  $^{153}\text{Sm}$ -FAPI-46. Although, one case is no proof of general efficacy, hopefully this study encourages further exploration of FAPI-based radionuclide therapy against soft tissue sarcoma.

Theranostics describes a close connection between diagnostics and consequent therapy. The term was probably first used in 1998 by John Funkhouser, and of course, this concept is not new in the nuclear medicine field [16]. It has been used for decades to treat benign and malignant thyroid diseases [146]. Moreover, in recent years, theranostics has been successfully applied to many other malignancies, including neuroendocrine tumors and

prostate cancer in particular. Radionuclide therapy not only has a palliative effect but can also prolong progression-free and overall survival. FAP as a therapeutic target in cancer was proposed and implemented soon after its discovery. Its unique enzymatic activity, the different expression between tumor tissue and normal tissue, and the importance of FAP-positive stromal cells in shaping the tumor microenvironment make it a promising target to various solid tumors [23]. Since the stroma can account for up to 90% of the total tumor mass, stroma-targeted radionuclide therapy, breaking the tumor stroma barrier may increase tumor cell accessibility for pharmacologic, immunologic, or cell-based therapies [147, 148]. Additionally, simultaneous irradiation of CAFs and surrounding tumor cells may also be achieved through the crossfire effect. Furthermore, since FAP-expressing CAFs are known to be immunosuppressive, a combination with immunotherapy may produce a synergistic effect [6, 7].

To date, FAPI variants showed a relatively fast clearance from tumor sites, limiting the achievable radiation dose for therapeutic applications. Although many optimized structures have been developed, more studies are needed to verify the actual effectiveness of these FAP-directed radionuclide therapies [16]. In addition, the possible off-target effect on related proteases may occur in the application of radiolabeled FAPIs. In this regard, a parallel inhibition of DPP4 and/or DPP8/9 may significantly contribute to the immunomodulatory effects [149, 150]. One thing to keep in mind is that since FAP-targeted strategy may not be suitable for eradicating individually dispersed tumor cells that have not induced a strong stromal reaction, implementing this method shortly after surgical removal of tumors with therapeutic purposes may be problematic [23]. FAP expression varies even among tumor types that are known to be generally FAP-positive. The optimal timing and combination of FAP-targeting approaches with current therapeutic paradigms is yet another challenge. Therefore, it is critical for future clinical studies to be of precise prospective design to compare the new FAPI-based approaches with standard treatments.

## Conclusion and future perspectives

The scientists who developed and optimized FAPIs and the researchers who evaluated FAPIs' value in early clinical trials have made exceptional contributions. Based on the early scientific evidence, FAPI-PET imaging may open a new chapter in molecular imaging in oncological and non-oncological diseases (Table 1 and Fig. 11). Overall, considering radiotracer uptake and tumor-to-background uptake ratio, compared to  $^{18}\text{F}$ -FDG-PET, FAPI-PET usually demonstrated an equal or higher detection rate of primary tumors and/or metastatic lesions, particularly in nasopharyngeal carcinoma, breast cancer, gastrointestinal tumors, and liver tumors. However, the most exciting aspect is its potential use as a theranostic tool, which might revolutionize the scope of radionuclide therapy and theranostics in the future. Although the available literature is encouraging, suggesting that FAPI outperforms  $^{18}\text{F}$ -FDG in various cancers, we emphasize that these studies have several limitations and are still preliminary, warranting further studies and trials. The limitations include (1) the patient populations were relatively small and heterogeneous; (2) most of the investigations were characteristic of moderate-to-low  $^{18}\text{F}$ -FDG-avid diseases, and the possible publication bias; (3) not all positive findings were confirmed histopathologically; and (4) follow-up time was relatively short. Notably, growing evidence has shown that



radiolabeled FAPI was not more tumor-specific than  $^{18}\text{F}$ -FDG (Table 2). Many cases of  $^{68}\text{Ga}$ -FAPI variant imaging in non-cancer patients have been reported, and some of them were found by accident in patients during a tumor scan. Although, this phenomenon suggests that FAPI is a nonspecific tumor agent and highlights its potential value in benign diseases. Meanwhile, nuclear medicine clinicians should be aware of this potential pitfall when evaluating  $^{68}\text{Ga}$ -FAPI imaging. Moreover, clinical studies are usually performed to evaluate the performance of  $^{68}\text{Ga}$ -FAPI variants and  $^{18}\text{F}$ -FDG at certain stages of tumor progression rather than the longitudinal imaging of patients with a series of PET scans. In addition, researchers have found that stromal FAP intensity was negatively correlated to tumor stage and xenografted tumor sizes; FAP-dependent pathways may play a leading role in the early development of tumors but may be diluted and diminished as other growth-promoting pathways predominate [151]. Since FAP has expressed different profiles in tumor development, it is premature to conclude that  $^{68}\text{Ga}$ -FAPI outperformed  $^{18}\text{F}$ -FDG for the entire tumor metastatic process, or it is hard to determine at which certain stage  $^{68}\text{Ga}$ -FAPI is more sensitive.

As a matter of fact,  $^{18}\text{F}$ -FDG accumulates in acute inflammation, whereas in recent studies, possibly due to a fibrotic reaction and FAP activation in chronic inflammation, increased radiolabeled FAPI uptake has been demonstrated. At the moment, FAPI-based imaging will not end the hegemony of  $^{18}\text{F}$ -FDG in oncology yet [152, 153]. Based on the available evidence, FAPI PET imaging is more accurately positioned as “not a replacement but a supplement” to  $^{18}\text{F}$ -FDG. Well-designed studies, including head-to-head comparisons, more extensive studies, ultimately randomized trials, and histopathological examinations, are needed to explore FAP-targeted applications’ diagnostic or therapeutic performance and clarify its usefulness in each disease and clinical setting.

## Funding

The authors are grateful for the financial support from the National Natural Science Foundation of China (No. 82030052), the University of Wisconsin—Madison, and the National Institutes of Health (P30CA014520).

## References

1. Hicks RJ, Roselt PJ, Kallur KG, Tohill RW, Mileshkin L. 2020 State-of-the-art: FAPI PET/CT-will it end the hegemony of FDG in oncology? *J Nucl Med.* 10.2967/jnumed.120.256271
2. Sanli Y, Garg I, Kandathil A, Kendi T, Zanetti MJB, Kuyumcu S, et al. Neuroendocrine tumor diagnosis and management: (68)Ga-DOTATATE PET/CT. *AJR Am J Roentgenol.* 2018;211:267–77. 10.2214/AJR.18.19881. [PubMed: 29975116]
3. Radzina M, Tirane M, Roznere L, Zemniece L, Dronka L, Kalnina M, et al. Accuracy of (68)Ga-PSMA-11 PET/CT and multiparametric MRI for the detection of local tumor and lymph node metastases in early biochemical recurrence of prostate cancer. *Am J Nucl Med Mol Imaging.* 2020;10:106–18. [PubMed: 32419979]
4. Hofman MS, Lawrentschuk N, Francis RJ, Tang C, Vela I, Thomas P, et al. Prostate-specific membrane antigen PET-CT in patients with high-risk prostate cancer before curative-intent surgery or radiotherapy (proPSMA): a prospective, randomised, multicentre study. *Lancet.* 2020;395:1208–16. 10.1016/S0140-6736(20)30314-7. [PubMed: 32209449]
5. Altmann A, Haberkorn U, Siveke J. The latest developments in imaging of fibroblast activation protein. *J Nucl Med.* 2021;62:160–7. 10.2967/jnumed.120.244806. [PubMed: 33127618]

6. Meyer C, Dahlbom M, Lindner T, Vauclin S, Mona C, Slavik R, et al. Radiation Dosimetry and Biodistribution of (68) Ga-FAPI-46 PET Imaging in Cancer Patients. *J Nucl Med*. 2020;61:1171–7. 10.2967/jnumed.119.236786. [PubMed: 31836685]
7. Lindner T, Loktev A, Giesel F, Kratochwil C, Altmann A, Haberkorn U. Targeting of activated fibroblasts for imaging and therapy. *EJNMMI Radiopharm Chem*. 2019;4:16. 10.1186/s41181-019-0069-0. [PubMed: 31659499]
8. Loktev A, Lindner T, Mier W, Debus J, Altmann A, Jager D, et al. A Tumor-imaging method targeting cancer-associated fibroblasts. *J Nucl Med*. 2018;59:1423–9. 10.2967/jnumed.118.210435. [PubMed: 29626120]
9. Lamprecht S, Sigal-Batikoff I, Shany S, Abu-Freha N, Ling E, Delinasios GJ, et al. Teaming up for trouble: cancer cells, transforming growth factor-beta1 signaling and the epigenetic corruption of stromal naive fibroblasts. *Cancers (Basel)*. 2018;10. 10.3390/cancers10030061.
10. Bu L, Baba H, Yoshida N, Miyake K, Yasuda T, Uchihara T, et al. Biological heterogeneity and versatility of cancer-associated fibroblasts in the tumor microenvironment. *Oncogene*. 2019;38:4887–901. 10.1038/s41388-019-0765-y. [PubMed: 30816343]
11. Egger C, Cannel C, Gerard C, Suply T, Ksiazek I, Jarman E, et al. Effects of the fibroblast activation protein inhibitor, PT100, in a murine model of pulmonary fibrosis. *Eur J Pharmacol*. 2017;809:64–72. 10.1016/j.ejphar.2017.05.022. [PubMed: 28506908]
12. Uitte de Willige S, Malfliet JJ, Janssen HL, Leebeek FW, Rijken DC. Increased N-terminal cleavage of alpha-2-antiplasmin in patients with liver cirrhosis. *J Thromb Haemost*. 2013;11:2029–36. 10.1111/jth.12396. [PubMed: 24034420]
13. Hamson EJ, Keane FM, Tholen S, Schilling O, Gorrell MD. Understanding fibroblast activation protein (FAP): substrates, activities, expression and targeting for cancer therapy. *Proteomics Clin Appl*. 2014;8:454–63. 10.1002/prca.201300095. [PubMed: 24470260]
14. Zhang X, Song W, Qin C, Song Y, Liu F, Hu F, et al. Uterine uptake of 68Ga-FAPI-04 in uterine pathology and physiology. *Clin Nucl Med*. 2022;47:7–13. 10.1097/RLU.0000000000003968. [PubMed: 34874344]
15. Keane FM, Yao TW, Seelk S, Gall MG, Chowdhury S, Poplawski SE, et al. Quantitation of fibroblast activation protein (FAP)-specific protease activity in mouse, baboon and human fluids and organs. *FEBS Open Bio*. 2013;4:43–54. 10.1016/j.fob.2013.12.001.
16. Langbein T, Weber WA, Eiber M. Future of theranostics: an outlook on precision oncology in nuclear medicine. *J Nucl Med*. 2019;60:13S–S19. 10.2967/jnumed.118.220566. [PubMed: 31481583]
17. Welt S, Divgi CR, Scott AM, Garin-Chesa P, Finn RD, Graham M, et al. Antibody targeting in metastatic colon cancer: a phase I study of monoclonal antibody F19 against a cell-surface protein of reactive tumor stromal fibroblasts. *J Clin Oncol*. 1994;12:1193–203. 10.1200/JCO.1994.12.6.1193. [PubMed: 8201382]
18. Loeffler M, Krüger JA, Niethammer AG, Reisfeld RA. Targeting tumor-associated fibroblasts improves cancer chemotherapy by increasing intratumoral drug uptake. *J Clin Invest*. 2006;116:1955–62. 10.1172/JCI26532. [PubMed: 16794736]
19. Ostermann E, Garin-Chesa P, Heider KH, Kalat M, Lamche H, Puri C, et al. Effective immunoconjugate therapy in cancer models targeting a serine protease of tumor fibroblasts. *Clin Cancer Res*. 2008;14:4584–92. 10.1158/1078-0432. [PubMed: 18628473]
20. Wang LC, Lo A, Scholler J, Sun J, Majumdar RS, Kapoor V, et al. Targeting fibroblast activation protein in tumor stroma with chimeric antigen receptor T cells can inhibit tumor growth and augment host immunity without severe toxicity. *Cancer Immunol Res*. 2014;2:154–66. 10.1158/2326-6066. [PubMed: 24778279]
21. Chen M, Lei X, Shi C, Huang M, Li X, Wu B, et al. Pericyte-targeting prodrug overcomes tumor resistance to vascular disrupting agents. *J Clin Invest*. 2017;127:3689–701. 10.1172/JCI94258. [PubMed: 28846068]
22. Teichgraber V, Monasterio C, Chaitanya K, Boger R, Gordon K, Dieterle T, et al. Specific inhibition of fibroblast activation protein (FAP)-alpha prevents tumor progression in vitro. *Adv Med Sci*. 2015;60:264–72. 10.1016/j.advms.2015.04.006. [PubMed: 26057860]

23. Busek P, Mateu R, Zubal M, Kotackova L, Sedo A. Targeting fibroblast activation protein in cancer — prospects and caveats. *Front Biosci (Landmark Ed)*. 2018;23:1933–68. 10.2741/4682. [PubMed: 29772538]
24. Meletta R, Muller Herde A, Chiotellis A, Isa M, Rancic Z, Borel N, et al. Evaluation of the radiolabeled boronic acid-based FAP inhibitor MIP-1232 for atherosclerotic plaque imaging. *Molecules*. 2015;20:2081–99. 10.3390/molecules20022081. [PubMed: 25633335]
25. Xu M, Zhang P, Ding J, Chen J, Huo L, Liu Z. Albumin binder-conjugated fibroblast activation protein inhibitor radiopharmaceuticals for cancer therapy. *J Nucl Med*. 2021;jnumed.121.262533. 10.2967/jnumed.121.262533.
26. Zhang P Xu M Ding J Chen J Zhang T Huo L Liu Z 2021 Fatty acid-conjugated radiopharmaceuticals for fibroblast activation protein-targeted radiotherapy *Eur J Nucl Med Mol Imaging* 10.1007/s00259-021-05591-x
27. Giesel FL, Kratochwil C, Lindner T, Marschalek MM, Loktev A, Lehnert W, et al. (68)Ga-FAPI PET/CT: Biodistribution and preliminary dosimetry estimate of 2 DOTA-containing FAP-targeting agents in patients with various cancers. *J Nucl Med*. 2019;60:386–92. 10.2967/jnumed.118.215913. [PubMed: 30072500]
28. Gourd E New radiotracer shows impressive diagnostic potential. *Lancet Oncol*. 2019;20: e353. 10.1016/S1470-2045(19)30422-X. [PubMed: 31204238]
29. Pang Y, Zhao L, Luo Z, Hao B, Wu H, Lin Q, et al. Comparison of (68)Ga-FAPI and (18)F-FDG uptake in gastric, duodenal, and colorectal cancers. *Radiology*. 2021;298:393–402. 10.1148/radiol.2020203275. [PubMed: 33258746]
30. Ferdinandus J, Kessler L, Hirmas N, Trajkovic-Arsic M, Hamacher R, Umutlu L, et al. Equivalent tumor detection for early and late FAPI-46 PET acquisition. *Eur J Nucl Med Mol Imaging*. 2021;48:3221–7. 10.1007/s00259-021-05266-7. [PubMed: 33620560]
31. Toms J, Kogler J, Maschauer S, Daniel C, Schmidkonz C, Kuwert T, et al. Targeting fibroblast activation protein: radiosynthesis and preclinical evaluation of an (18)F-labeled FAP inhibitor. *J Nucl Med*. 2020;61:1806–13. 10.2967/jnumed.120.242958. [PubMed: 32332144]
32. Wang S, Zhou X, Xu X, Ding J, Liu S, Hou X, et al. Clinical translational evaluation of Al(18)F-NOTA-FAPI for fibroblast activation protein-targeted tumour imaging. *Eur J Nucl Med Mol Imaging*. 2021;48:4259–71. 10.1007/s00259-021-05470-5. [PubMed: 34165601]
33. Kratochwil C, Flechsig P, Lindner T, Abderrahim L, Altmann A, Mier W, et al. (68)Ga-FAPI PET/CT: tracer uptake in 28 different kinds of cancer. *J Nucl Med*. 2019;60:801–5. 10.2967/jnumed.119.227967. [PubMed: 30954939]
34. Sharma P, Singh SS, Gayana S. Fibroblast activation protein inhibitor PET/CT: a promising molecular imaging tool. *Clin Nucl Med*. 2021;46:e141–50. 10.1097/RLU.0000000000003489. [PubMed: 33351507]
35. Lindner T, Loktev A, Altmann A, Giesel F, Kratochwil C, Debus J, et al. Development of quinoline-based theranostic ligands for the targeting of fibroblast activation protein. *J Nucl Med*. 2018;59:1415–22. 10.2967/jnumed.118.210443. [PubMed: 29626119]
36. Loktev A, Lindner T, Burger EM, Altmann A, Giesel F, Kratochwil C, et al. Development of fibroblast activation protein-targeted radiotracers with improved tumor retention. *J Nucl Med*. 2019;60:1421–9. 10.2967/jnumed.118.224469. [PubMed: 30850501]
37. Watabe T, Liu Y, Kaneda-Nakashima K, Shirakami Y, Lindner T, Ooe K, et al. Theranostics targeting fibroblast activation protein in the tumor stroma: (64)Cu- and (225)Ac-labeled FAPI-04 in pancreatic cancer xenograft mouse models. *J Nucl Med*. 2020;61:563–9. 10.2967/jnumed.119.233122. [PubMed: 31586001]
38. Varasteh Z, Mohanta S, Robu S, Braeuer M, Li Y, Omidvari N, et al. Molecular imaging of fibroblast activity after myocardial infarction using a (68)Ga-labeled fibroblast activation protein inhibitor, FAPI-04. *J Nucl Med*. 2019;60:1743–9. 10.2967/jnumed.119.226993. [PubMed: 31405922]
39. Qin C Liu F Huang J Ruan W Liu Q Gai Y et al. 2021 A head-to-head comparison of (68)Ga-DOTA-FAPI-04 and (18)F-FDG PET/MR in patients with nasopharyngeal carcinoma: a prospective study *Eur J Nucl Med Mol Imaging* 10.1007/s00259-021-05255-w

40. Zhao L, Pang Y, Zheng H, Han C, Gu J, Sun L, et al. Clinical utility of [68Ga]Ga-labeled fibroblast activation protein inhibitor (FAPI) positron emission tomography/computed tomography for primary staging and recurrence detection in nasopharyngeal carcinoma. *Eur J Nucl Med Mol Imaging*. 2021;48:3606–17. 10.1007/s00259-021-05336-w. [PubMed: 33792760]
41. Millul J, Bassi G, Mock J, Elsayed A, Pellegrino C, Zana A, et al. An ultra-high-affinity small organic ligand of fibroblast activation protein for tumor-targeting applications. *Proc Natl Acad Sci U S A*. 2021;118: e2101852118. 10.1073/pnas.2101852118. [PubMed: 33850024]
42. Giesel FL, Adeberg S, Syed M, Lindner T, Jiménez-Franco LD, Mavriopoulou E, et al. FAPI-74 PET/CT using either 18F-AIF or Cold-Kit 68Ga labeling: biodistribution, radiation dosimetry, and tumor delineation in lung cancer patients. *J Nucl Med*. 2021;62:201–7. 10.2967/jnumed.120.245084. [PubMed: 32591493]
43. Louis DN, Perry A, Wesseling P, Brat DJ, Cree IA, Figarella-Branger D, et al. The 2021 WHO Classification of Tumors of the Central Nervous System: a summary. *Neuro Oncol*. 2021;23:1231–51. 10.1093/neuonc/noab106. [PubMed: 34185076]
44. Aimes RT, Zijlstra A, Hooper JD, Ogbourne SM, Sit ML, Fuchs S, et al. Endothelial cell serine proteases expressed during vascular morphogenesis and angiogenesis. *Thromb Haemost*. 2003;89:561–72. [PubMed: 12624642]
45. Busek P, Balaziova E, Matrasova I, Hilser M, Tomas R, Syrucek M, et al. Fibroblast activation protein alpha is expressed by transformed and stromal cells and is associated with mesenchymal features in glioblastoma. *Tumour Biol*. 2016;37:13961–71. 10.1007/s13277-016-5274-9. [PubMed: 27492457]
46. Rohrich M, Loktev A, Wefers AK, Altmann A, Paech D, Adeberg S, et al. IDH-wildtype glioblastomas and grade III/IV IDH-mutant gliomas show elevated tracer uptake in fibroblast activation protein-specific PET/CT. *Eur J Nucl Med Mol Imaging*. 2019;46:2569–80. 10.1007/s00259-019-04444-y. [PubMed: 31388723]
47. Röhrich M, Floca R, Loi L, Adeberg S, Windisch P, Giesel FL, et al. FAP-specific PET signaling shows a moderately positive correlation with relative CBV and no correlation with ADC in 13 IDH wildtype glioblastomas. *Eur J Radiol*. 2020;127: 109021. 10.1016/j.ejrad.2020.109021. [PubMed: 32344293]
48. Lin JJ, Chuang CP, Lin JY, Huang FT, Huang CW. Rational design, pharmacomodulation, and synthesis of [(68)Ga]Ga-Alb-FAPt-01, a selective tumor-associated fibroblast activation protein tracer for PET imaging of glioma. *ACS Sens*. 2021;6:3424–35. 10.1021/acssensors.1c01316. [PubMed: 34415143]
49. Chen YP CA, Le QT, Blanchard P, Sun Y, Ma J. Nasopharyngeal carcinoma; 2019.
50. Colevas AD, Yom SS, Pfister DG, Spencer S, Adelstein D, Adkins D, et al. NCCN Guidelines Insights: head and neck cancers, Version 1.2018. *J Natl Compr Canc Netw*. 2018;16:479–90. 10.6004/jnccn.2018.0026. [PubMed: 29752322]
51. Shang Q, Zhao L, Pang Y, Yu Y, Chen H. 68Ga-FAPI PET/CT Distinguishes the reactive lymph nodes from tumor metastatic lymph nodes in a patient with nasopharyngeal carcinoma. *Clin Nucl Med*. 2021. 10.1097/RLU.0000000000003939.
52. Gu B Xu X Zhang J Ou X Xia Z Guan Q et al. 2021 The Added Value of (68)Ga-FAPI-04 PET/CT in patients with head and neck cancer of unknown primary with (18)F-FDG negative findings *J Nucl Med* 10.2967/jnumed.121.262790
53. Siegel RL, Miller KD, Jemal A. Cancer statistics, 2020. *CA Cancer J Clin*. 2020;70:7–30. 10.3322/caac.21590. [PubMed: 31912902]
54. Rohren EM, Turkington TG, Coleman RE. Clinical applications of PET in oncology. *Radiology*. 2004;231:305–32. 10.1148/radiol.2312021185. [PubMed: 15044750]
55. Guo W, Chen H. (68)Ga FAPI PET/CT imaging in peritoneal carcinomatosis. *Radiology*. 2020;297:521. 10.1148/radiol.2020202469. [PubMed: 33048036]
56. Zhao L, Pang Y, Luo Z, Fu K, Yang T, Zhao L, et al. Role of [(68) Ga]Ga-DOTA-FAPI-04 PET/CT in the evaluation of peritoneal carcinomatosis and comparison with [(18)F]-FDG PET/CT. *Eur J Nucl Med Mol Imaging*. 2021;48:1944–55. 10.1007/s00259-020-05146-6. [PubMed: 33415432]

57. Kuten J, Levine C, Shamni O, Pelles S, Wolf I, Lahat G et al. 2021 Head-to-head comparison of [(68)Ga]Ga-FAPI-04 and [(18)F]-FDG PET/CT in evaluating the extent of disease in gastric adenocarcinoma. *Eur J Nucl Med Mol Imaging* 10.1007/s00259-021-05494-x
58. Jiang D, Chen X, You Z, Wang H, Zhang X, Li X et al. 2021 Comparison of [(68) Ga]Ga-FAPI-04 and [(18)F]-FDG for the detection of primary and metastatic lesions in patients with gastric cancer: a bicentric retrospective study. *Eur J Nucl Med Mol Imaging* 10.1007/s00259-021-05441-w
59. Qin C, Shao F, Gai Y, Liu Q, Ruan W, Liu F et al. 2021 (68) Ga-DOTA-FAPI-04 PET/MR in the evaluation of gastric carcinomas: comparison with (18)F-FDG PET/CT. *J Nucl Med* 10.2967/jnumed.120.258467
60. Koerber SA, Staudinger F, Kratochwil C, Adeberg S, Haefner MF, Ungerechts G, et al. The role of (68)Ga-FAPI PET/CT for patients with malignancies of the lower gastrointestinal tract: first clinical experience. *J Nucl Med*. 2020;61:1331–6. 10.2967/jnumed.119.237016. [PubMed: 32060216]
61. Forner A, Reig M, Bruix J. Hepatocellular carcinoma. *Lancet*. 2018;391:1301–14. 10.1016/S0140-6736(18)30010-2. [PubMed: 29307467]
62. Mertens JC, Rizvi S, Gores GJ. Targeting cholangiocarcinoma. *Biochim Biophys Acta Mol Basis Dis*. 2018;1864:1454–60. 10.1016/j.bbdis.2017.08.027. [PubMed: 28844952]
63. Shi X, Xing H, Yang X, Li F, Yao S, Congwei J et al. 2020 Comparison of PET imaging of activated fibroblasts and (18)F-FDG for diagnosis of primary hepatic tumours: a prospective pilot study. *Eur J Nucl Med Mol Imaging* 10.1007/s00259-020-05070-9
64. Guo W, Pang Y, Yao L, Zhao L, Fan C, Ke J, et al. Imaging fibroblast activation protein in liver cancer: a single-center post hoc retrospective analysis to compare [(68)Ga]Ga-FAPI-04 PET/CT versus MRI and [(18)F]-FDG PET/CT. *Eur J Nucl Med Mol Imaging*. 2021;48:1604–17. 10.1007/s00259-020-05095-0. [PubMed: 33179149]
65. Wang H, Zhu W, Ren S, Kong Y, Huang Q, Zhao J, et al. (68) Ga-FAPI-04 versus (18)F-FDG PET/CT in the detection of hepatocellular carcinoma. *Front Oncol*. 2021;11: 693640. 10.3389/fonc.2021.693640. [PubMed: 34249748]
66. Shi X, Xing H, Yang X, Li F, Yao S, Zhang H, et al. Fibroblast imaging of hepatic carcinoma with (68)Ga-FAPI-04 PET/CT: a pilot study in patients with suspected hepatic nodules. *Eur J Nucl Med Mol Imaging*. 2021;48:196–203. 10.1007/s00259-020-04882-z. [PubMed: 32468254]
67. Pang Y, Hao B, Shang Q, Sun L, Chen H. Comparison of 68Ga-FAPI and 18F-FDG PET/CT in a patient with cholangiocellular carcinoma: a case report. *Clin Nucl Med*. 2020;45:566–7. 10.1097/RLU.0000000000003056. [PubMed: 32371618]
68. Zhao L, Gu J, Fu K, Lin Q, Chen H. 68Ga-FAPI PET/CT in assessment of liver nodules in a cirrhotic patient. *Clin Nucl Med*. 2020;45:e430–2. 10.1097/RLU.0000000000003015. [PubMed: 32332301]
69. Tempero MA, Malafa MP, Al-Hawary M, Behrman SW, Benson AB, Cardin DB, et al. Pancreatic Adenocarcinoma, Version 2.2021, NCCN Clinical Practice Guidelines in Oncology. *J Natl Compr Canc Netw*. 2021;19:439–57. 10.6004/jnccn.2021.0017. [PubMed: 33845462]
70. Zhang L, Sanagapalli S, Stoita A. Challenges in diagnosis of pancreatic cancer. *World J Gastroenterol*. 2018;24:2047–60. 10.3748/wjg.v24.i19.2047. [PubMed: 29785074]
71. Pang Y, Zhao L, Shang Q, Meng T, Zhao L, Feng L et al. 2021 Positron emission tomography and computed tomography with [(68)Ga]Ga-fibroblast activation protein inhibitors improves tumor detection and staging in patients with pancreatic cancer. *Eur J Nucl Med Mol Imaging* 10.1007/s00259-021-05576-w
72. Zhang X, Song W, Qin C, Liu F, Lan X. Non-malignant findings of focal (68)Ga-FAPI-04 uptake in pancreas. *Eur J Nucl Med Mol Imaging*. 2021;48:2635–41. 10.1007/s00259-021-05194-6. [PubMed: 33452634]
73. Cheng Z, Zou S, Cheng S, Song S, Zhu X. Comparison of 18F-FDG, 68Ga-FAPI, and 68Ga-DOTATATE PET/CT in a patient with pancreatic neuroendocrine tumor. *Clin Nucl Med*. 2021;46:764–5. 10.1097/RLU.0000000000003763. [PubMed: 34132674]
74. Komek H, Gundogan C, Can C. 68Ga-FAPI PET/CT Versus 68Ga-DOTATATE PET/CT in the evaluation of a patient with neuroendocrine tumor. *Clin Nucl Med*. 2021;46:e290–2. 10.1097/RLU.0000000000003490. [PubMed: 33351508]



75. Mankoff DA, Sellmyer MA. PET of fibroblast-activation protein for breast cancer diagnosis and staging. *Radiology*. 2021;212098. 10.1148/radiol.2021212098.
76. Backhaus P, Burg MC, Roll W, Buther F, Breyholz HJ, Weigel S, et al. Simultaneous FAPI PET/MRI targeting the fibroblast-activation protein for breast cancer. *radiology*. 2021;204677. 10.1148/radiol.2021204677.
77. Elboga U, Sahin E, Kus T, Cayirli YB, Aktas G, Uzun E, et al. Superiority of (68)Ga-FAPI PET/CT scan in detecting additional lesions compared to (18)FDG PET/CT scan in breast cancer. *Ann Nucl Med*. 2021;35:1321–31. 10.1007/s12149-021-01672-x. [PubMed: 34436740]
78. Komek H, Gundogan C, Etem H, Can C. A case with (68)Ga-FAPI positive and (18)F-FDG negative breast cancer. *Mol Imaging Radionucl Ther*. 2021;30:201–4. 10.4274/mirt.galenos.2021.69926. [PubMed: 34661066]
79. Wang Q Tang W Cai L Chen F 2021 Non-18F-FDG-avid intrahepatic metastasis of breast cancer revealed by 68Ga-FAPI PET/CT *ClinNucl Med* 10.1097/RLU.0000000000003905
80. Pang Y, Zhao L, Chen H. 68Ga-FAPI outperforms 18F-FDG PET/CT in identifying bone metastasis and peritoneal carcinomatosis in a patient with metastatic breast cancer. *Clin Nucl Med*. 2020;45:913–5. 10.1097/RLU.0000000000003263. [PubMed: 32910045]
81. Gundogan C, Guzel Y, Can C, Alabalik U, Komek H. False-Positive 68Ga-fibroblast activation protein-specific inhibitor uptake of benign lymphoid tissue in a patient with breast cancer. *Clin Nucl Med*. 2021;46:e433–5. 10.1097/RLU.0000000000003594. [PubMed: 33782295]
82. Zheng S, Chen Y, Zhu Y, Yao S, Miao W. Both [(68)Ga]Ga-FAPI and [(18)F]FDG PET/CT missed bone metastasis in a patient with breast cancer. *Eur J Nucl Med Mol Imaging*. 2021;48:4519–20. 10.1007/s00259-021-05453-6. [PubMed: 34131802]
83. Dendl K, Koerber SA, Finck R, Mokoala KMG, Staudinger F, Schillings L, et al. (68)Ga-FAPI-PET/CT in patients with various gynecological malignancies. *Eur J Nucl Med Mol Imaging*. 2021;48:4089–100. 10.1007/s00259-021-05378-0. [PubMed: 34050777]
84. Heller SL, Young Lin LL, Melsaether AN, Moy L, Gao Y. Hormonal effects on breast density, fibroglandular tissue, and background parenchymal enhancement. *Radiographics*. 2018;38:983–96. 10.1148/rg.2018180035. [PubMed: 29856684]
85. Isik EG Has-Simsek D Sanli O Sanli Y Kuyumcu S 2021 Fibroblast activation protein-targeted PET imaging of metastatic castration-resistant prostate cancer compared with 68Ga-PSMA and 18F-FDG PET/CT *ClinNucl Med* 10.1097/RLU.0000000000003837
86. Kesch C Yirga L Dendl K Handke A Darr C Krafft U et al. 2021 High fibroblast-activation-protein expression in castration-resistant prostate cancer supports the use of FAPI-molecular theranostics *Eur J Nucl Med Mol Imaging* 10.1007/s00259-021-05423-y
87. Wu J, Wang Y, Liao T, Rao Z, Gong W, Ou L, et al. Comparison of the relative diagnostic performance of [(68)Ga] Ga-DOTA-FAPI-04 and [(18)F]FDG PET/CT for the detection of bone metastasis in patients with different cancers. *Front Oncol*. 2021;11: 737827. 10.3389/fonc.2021.737827. [PubMed: 34604078]
88. Ou L, Wu J, Wu J, Mou C, Zhang C. Follicular thyroid adenoma showing avid uptake on 68Ga-DOTA-FAPI-04 PET/CT. *Clin Nucl Med*. 2021;46:840–1. 10.1097/RLU.0000000000003762. [PubMed: 34172606]
89. Haugen BR, Alexander EK, Bible KC, Doherty GM, Mandel SJ, Nikiforov YE, et al. 2015 American Thyroid Association Management Guidelines for Adult Patients with Thyroid Nodules and Differentiated Thyroid Cancer: The American Thyroid Association Guidelines Task Force on Thyroid Nodules and Differentiated Thyroid Cancer. *Thyroid*. 2016;26:1–133. 10.1089/thy.2015.0020. [PubMed: 26462967]
90. van Dijk D, Plukker JT, Phan HT, Muller Kobold AC, van der Horst-Schrivers AN, Jansen L, et al. 18-fluorodeoxyglucose positron emission tomography in the early diagnostic workup of differentiated thyroid cancer patients with a negative post-therapeutic iodine scan and detectable thyroglobulin. *Thyroid*. 2013;23:1003–9. 10.1089/thy.2012.0498. [PubMed: 23517405]
91. Wu J, Ou L, Zhang C. Comparison of (68)Ga-FAPI and (18) F-FDG PET/CT in metastases of papillary thyroid carcinoma. *Endocrine*. 2021;73:767–8. 10.1007/s12020-021-02668-3. [PubMed: 33674912]



92. Fu H, Fu J, Huang J, Su X, Chen H. 68Ga-FAPI PET/CT in thyroid cancer with thyroglobulin elevation and negative iodine scintigraphy. *Clin Nucl Med*. 2021;46:427–30. 10.1097/RLU.0000000000003569. [PubMed: 33661204]
93. Fu H, Fu J, Huang J, Pang Y, Chen H. 68Ga-FAPI PET/CT versus 18F-FDG PET/CT for detecting metastatic lesions in a case of radioiodine-refractory differentiated thyroid cancer. *Clin Nucl Med*. 2021;46:940–2. 10.1097/RLU.0000000000003730. [PubMed: 34034326]
94. Zhao L, Pang Y, Lin Q, Chen H. Cardiac angiosarcoma detected using 68Ga-fibroblast activation protein inhibitor positron emission tomography/magnetic resonance. *Eur Heart J*. 2021;42:1276. 10.1093/eurheartj/ehaa931. [PubMed: 33320948]
95. Wang G, Jin X, Zhu H, Wang S, Ding J, Zhang Y, et al. (68) Ga-NOTA-FAPI-04 PET/CT in a patient with primary gastric diffuse large B cell lymphoma: comparisons with [(18)F] FDG PET/CT. *Eur J Nucl Med Mol Imaging*. 2021;48:647–8. 10.1007/s00259-020-04946-0. [PubMed: 32632460]
96. Zhang Y, Cai J, Lin Z, Yao S, Miao W. Primary central nervous system lymphoma revealed by 68Ga-FAPI and 18F-FDG PET/CT. *Clin Nucl Med*. 2021;46:e421–3. 10.1097/RLU.0000000000003517. [PubMed: 33512949]
97. Luo Y, Pan Q, Yang H, Peng L, Zhang W, Li F. Fibroblast activation protein-targeted PET/CT with (68)Ga-FAPI for imaging IgG4-related disease: comparison to (18)F-FDG PET/CT. *J Nucl Med*. 2021;62:266–71. 10.2967/jnumed.120.244723. [PubMed: 32513902]
98. Pan Q, Luo Y, Zhang W. Recurrent immunoglobulin G4-related disease shown on 18F-FDG and 68Ga-FAPI PET/CT. *Clin Nucl Med*. 2020;45:312–3. 10.1097/RLU.0000000000002919. [PubMed: 31977476]
99. Shou Y, Xue Q, Yuan J, Zhao J. (68)Ga-FAPI-04 PET/MR is helpful in differential diagnosis of pancreatitis from pancreatic malignancy compared to (18)F-FDG PET/CT: a case report. *Eur J Hybrid Imaging*. 2021;5:12. 10.1186/s41824-021-00106-1. [PubMed: 34181149]
100. Qin C, Yang L, Ruan W, Shao F, Lan X. Immunoglobulin G4-related sclerosing cholangitis revealed by 68Ga-FAPI PET/MR. *Clin Nucl Med*. 2021;46:419–21. 10.1097/RLU.0000000000003552. [PubMed: 33630803]
101. Luo Y, Pan Q, Zhang W. IgG4-related disease revealed by (68)Ga-FAPI and (18)F-FDG PET/CT. *Eur J Nucl Med Mol Imaging*. 2019;46:2625–6. 10.1007/s00259-019-04478-2. [PubMed: 31410541]
102. Schmidkonz C, Rauber S, Atzinger A, Agarwal R, Gotz TI, Soare A, et al. Disentangling inflammatory from fibrotic disease activity by fibroblast activation protein imaging. *Ann Rheum Dis*. 2020;79:1485–91. 10.1136/annrheumdis-2020-217408. [PubMed: 32719042]
103. Kessler L, Kupusovic J, Ferdinandus J, Hirmas N, Umutlu L, Zarrad F, et al. Visualization of fibroblast activation after myocardial infarction using 68Ga-FAPI PET. *Clin Nucl Med*. 2021;46:807–13. 10.1097/RLU.0000000000003745. [PubMed: 34477601]
104. Notohamiprodjo S, Nekolla SG, Robu S, Villagran Asiares A, Kupatt C, Ibrahim T, et al. Imaging of cardiac fibroblast activation in a patient after acute myocardial infarction using (68) Ga-FAPI-04. *J Nucl Cardiol*. 2021. 10.1007/s12350-021-02603-z.
105. Siebermair J, Kohler MI, Kupusovic J, Nekolla SG, Kessler L, Ferdinandus J, et al. Cardiac fibroblast activation detected by Ga-68 FAPI PET imaging as a potential novel biomarker of cardiac injury/remodeling. *J Nucl Cardiol*. 2021;28:812–21. 10.1007/s12350-020-02307-w. [PubMed: 32975729]
106. Heckmann MB, Reinhardt F, Finke D, Katus HA, Haberkorn U, Leuschner F, et al. Relationship between cardiac fibroblast activation protein activity by positron emission tomography and cardiovascular disease. *Circ Cardiovasc Imaging*. 2020;13:e010628. 10.1161/CIRCIMAGING.120.010628. [PubMed: 32912030]
107. Wang L, Zhang Z, Zhao Z, Yan C, Fang W. (68)Ga-FAPI right heart uptake in a patient with idiopathic pulmonary arterial hypertension. *J Nucl Cardiol*. 10.1007/s12350-020-02407-7
108. Chen BX, Xing HQ, Gong JN, Guo XJ, Xi XY, Yang YH, et al. 2021 Imaging of cardiac fibroblast activation in patients with chronic thromboembolic pulmonary hypertension. *Eur J Nucl Med Mol Imaging*. 10.1007/s00259-021-05577-9

109. Lin K, Chen X, Xue Q, Yao S, Miao W. 2021 Diffuse uptake of [(68)Ga]Ga-FAPI in the left heart in a patient with hypertensive heart disease by PET/CT. *J NuclCardiol* 10.1007/s12350-021-02646-2
110. Totzeck M, Siebermair J, Rassaf T, Rischpler C. Cardiac fibroblast activation detected by positron emission tomography/computed tomography as a possible sign of cardiotoxicity. *Eur Heart J*. 2020;41:1060. 10.1093/eurheartj/ehz736. [PubMed: 31630152]
111. Kupusovic J, Kessler L, Nekolla SG, Riesinger L, Weber MM, Ferdinandus J et al. 2021 Visualization of thermal damage using (68) Ga-FAPI-PET/CT after pulmonary vein isolation. *Eur J Nucl Med Mol Imaging* 10.1007/s00259-021-05612-9
112. Wang DY, Salem JE, Cohen JV, Chandra S, Menzer C, Ye F, et al. Fatal toxic effects associated with immune checkpoint inhibitors: a systematic review and meta-analysis. *JAMA Oncol*. 2018;4:1721–8. 10.1001/jamaoncol.2018.3923. [PubMed: 30242316]
113. Finke D, Heckmann MB, Herpel E, Katus HA, Haberkorn U, Leuschner F, et al. Early detection of checkpoint inhibitor-associated myocarditis using (68)Ga-FAPI PET/CT. *Front Cardiovasc Med*. 2021;8: 614997. 10.3389/fcvm.2021.614997. [PubMed: 33718446]
114. Lay AJ, Zhang HE, McCaughan GW, Gorrell MD. Fibroblast activation protein in liver fibrosis. *Front Biosci (Landmark Ed)*. 2019;24:1–17. 10.2741/4706. [PubMed: 30468644]
115. Xu T, Zhao Y, Ding H, Cai L, Zhou Z, Song Z, et al. [(68) Ga]Ga-DOTA-FAPI-04 PET/CT imaging in a case of prostate cancer with shoulder arthritis. *Eur J Nucl Med Mol Imaging*. 2021;48:1254–5. 10.1007/s00259-020-05028-x. [PubMed: 32901354]
116. Liu H, Chen Z, Yang X, Fu W, Chen Y. Increased 68Ga-FAPI uptake in chronic cholecystitis and degenerative osteophyte. *Clin Nucl Med*. 2021;46:601–2. 10.1097/RLU.0000000000003621. [PubMed: 33782317]
117. Liu H, Wang Y, Zhang W, Cai L, Chen Y. Elevated [(68) Ga]Ga-DOTA-FAPI-04 activity in degenerative osteophyte in a patient with lung cancer. *Eur J Nucl Med Mol Imaging*. 2021;48:1671–2. 10.1007/s00259-020-05090-5. [PubMed: 33184681]
118. Lin R, Lin Z, Zhang J, Yao S, Miao W. Increased 68Ga-FAPI-04 uptake in schmorl node in a patient with gastric cancer. *Clin Nucl Med*. 2021;46:700–2. 10.1097/RLU.0000000000003623. [PubMed: 33826575]
119. Wu J, Liu H, Ou L, Jiang G, Zhang C. FAPI Uptake in a vertebral body fracture in a patient with lung cancer: a FAPI imaging pitfall. *Clin Nucl Med*. 2021;46:520–2. 10.1097/RLU.0000000000003560. [PubMed: 33661208]
120. Lv Y, Lan X, Qin C. Incidental detection of sacral insufficiency fracture on 68Ga-FAPI PET/MR. *Clin Nucl Med*. 2021;46:1032–3. 10.1097/RLU.0000000000003898. [PubMed: 34524169]
121. Gungor S, Selcuk NA. 2021 Benign bone cyst mimicking bone metastasis demonstrated on 68Ga-FAPI. *ClinNucl Med* 10.1097/RLU.0000000000003796
122. Song Y, Qin C, Liu F, Lan X. Fibrous dysplasia mimicking skeletal metastasis on 68Ga-FAPI PET imaging. *Clin Nucl Med*. 2021;46:774–5. 10.1097/RLU.0000000000003671. [PubMed: 33883497]
123. Wang Y, Wu J, Liu L, Peng D, Chen Y. 2021 68Ga-FAPI-04 PET/CT imaging for fibrous dysplasia of the bone. *ClinNucl Med* 10.1097/RLU.0000000000003896
124. Yao L, Zhao L, Pang Y, Shang Q, Chen H. 2021 Increased 68Ga-FAPI uptake in ankylosing spondylitis in a patient with rectal cancer. *ClinNucl Med* 10.1097/RLU.0000000000003798
125. Yang X, Liu Y, Chen J, Chen Y, Liu H. 68Ga-FAPI PET/CT imaging of bastrup disease in a patient with esophageal cancer. *Clin Nucl Med*. 2021;46:1024–5. 10.1097/RLU.0000000000003902. [PubMed: 34524164]
126. ErolFenercioglu O, Beyhan E, Ergul N, Arslan E, Cermik TF. 2021 18F-FDG PET/CT and 68Ga-FAPI-4 PET/CT findings of bilateral knee osteoarthritis in a patient with uveal malignant melanoma. *Clin Nucl Med* 10.1097/RLU.0000000000003854
127. Zhou Y, He J, Chen Y. 2021 (68)Ga-FAPI PET/CT imaging in a patient with thyroiditis. *Endocrine* 10.1007/s12020-021-02605-4
128. Gu B, Luo Z, He X, Wang J, Song S. 68Ga-FAPI and 18F-FDG PET/CT images in a patient with extrapulmonary tuberculosis mimicking malignant tumor. *Clin Nucl Med*. 2020;45:865–7. 10.1097/RLU.0000000000003279. [PubMed: 32969904]

129. Hao B, Wu X, Pang Y, Sun L, Wu H, Huang W, et al. [(18)F]FDG and [(68)Ga]Ga-DOTA-FAPI-04 PET/CT in the evaluation of tuberculous lesions. *Eur J Nucl Med Mol Imaging*. 2021;48:651–2. 10.1007/s00259-020-04941-5. [PubMed: 32643006]
130. Wu S, Pang Y, Chen Y, Sun H, Chen H. 68Ga-DOTA-FAPI-04 PET/CT in Erdheim-Chester disease. *Clin Nucl Med*. 2021;46:258–60. 10.1097/RLU.0000000000003491. [PubMed: 33417343]
131. Luo Y Pan Q Xu H Zhang R Li J Li F 2020 Active uptake of (68)Ga-FAPI in Crohn's disease but not in ulcerative colitis *Eur J Nucl Med Mol Imaging* 10.1007/s00259-020-05129-7
132. Liu H, Wang Y, Zhang W, Cai L, Chen Y. Elevated 68Ga-FAPI activity in splenic hemangioma and pneumonia. *Clin Nucl Med*. 2021;46:694–6. 10.1097/RLU.0000000000003638. [PubMed: 33826568]
133. Zhou Y, Yang X, Liu H, Luo W, Liu H, Lv T, et al. Value of [(68) Ga]Ga-FAPI-04 imaging in the diagnosis of renal fibrosis. *Eur J Nucl Med Mol Imaging*. 2021;48:3493–501. 10.1007/s00259-021-05343-x. [PubMed: 33829416]
134. Syed M, Flechsig P, Liermann J, Windisch P, Staudinger F, Akbaba S, et al. Fibroblast activation protein inhibitor (FAPI) PET for diagnostics and advanced targeted radiotherapy in head and neck cancers. *Eur J Nucl Med Mol Imaging*. 2020;47:2836–45. 10.1007/s00259-020-04859-y. [PubMed: 32447444]
135. Conen P, Mottaghy FM. Is (68)Ga-DOTA-FAPI a new arrow in the quiver of dose painting in radiation dose planning in head and neck cancers? *Eur J Nucl Med Mol Imaging*. 2020;47:2718–20. 10.1007/s00259-020-04895-8. [PubMed: 32488339]
136. Windisch P, Röhrich M, Regnery S, Tonndorf-Martini E, Held T, Lang K, et al. Fibroblast activation protein (FAP) specific PET for advanced target volume delineation in glioblastoma. *Radiother Oncol*. 2020;150:159–63. 10.1016/j.radonc.2020.06.040. [PubMed: 32598977]
137. Rohrich M, Syed M, Liew DP, Giesel FL, Liermann J, Choyke PL, et al. (68)Ga-FAPI-PET/CT improves diagnostic staging and radiotherapy planning of adenoid cystic carcinomas — imaging analysis and histological validation. *Radiother Oncol*. 2021;160:192–201. 10.1016/j.radonc.2021.04.016. [PubMed: 33940087]
138. Ristau J, Giesel FL, Haefner MF, Staudinger F, Lindner T, Merkel A, et al. Impact of primary staging with fibroblast activation protein specific enzyme inhibitor (FAPI)-PET/CT on radio-oncologic treatment planning of patients with esophageal cancer. *Mol Imaging Biol*. 2020;22:1495–500. 10.1007/s11307-020-01548-y. [PubMed: 33063132]
139. Zhao L, Chen S, Chen S, Pang Y, Dai Y, Hu S, et al. 68Ga-fibroblast activation protein inhibitor PET/CT on gross tumour volume delineation for radiotherapy planning of oesophageal cancer. *Radiother Oncol*. 2021;158:55–61. 10.1016/j.radonc.2021.02.015. [PubMed: 33621587]
140. Liermann J, Syed M, Ben-Josef E, Schubert K, Schlampp I, Sprengel SD, et al. Impact of FAPI-PET/CT on target volume definition in radiation therapy of locally recurrent pancreatic cancer. *Cancers (Basel)*. 2021;13. 10.3390/cancers13040796.
141. Zhao L Niu B Fang J Pang Y Li S Xie C et al. 2021 Synthesis, preclinical evaluation, and a pilot clinical PET imaging study of (68)Ga-labeled FAPI dimer *J Nucl Med* 10.2967/jnumed.121.263016
142. Ballal S, Yadav MP, Kramer V, Moon ES, Roesch F, Tripathi M, et al. A theranostic approach of [(68)Ga]Ga-DOTA. SA.FAPi PET/CT-guided [(177)Lu]Lu-DOTA.SA.FAPi radionuclide therapy in an end-stage breast cancer patient: new frontier in targeted radionuclide therapy. *Eur J Nucl Med Mol Imaging*. 2021;48:942–4. 10.1007/s00259-020-04990-w. [PubMed: 32783111]
143. Ballal S Yadav MP Moon ES Roesch F Kumari S Agarwal S et al. 2021 Novel fibroblast activation protein inhibitor-based targeted theranostics for radioiodine refractory differentiated thyroid cancer patients: A Pilot Study *Thyroid* 10.1089/thy.2021.0412
144. Lindner T, Altmann A, Kramer S, Kleist C, Loktev A, Kratochwil C, et al. Design and development of (99m) Tc-labeled FAPI tracers for SPECT imaging and (188)Re therapy. *J Nucl Med*. 2020;61:1507–13. 10.2967/jnumed.119.239731. [PubMed: 32169911]
145. Kratochwil C, Giesel FL, Rathke H, Fink R, Dendl K, Debus J, et al. [(153)Sm]Samarium-labeled FAPI-46 radioligand therapy in a patient with lung metastases of a sarcoma. *Eur J Nucl Med Mol Imaging*. 2021;48:3011–3. 10.1007/s00259-021-05273-8. [PubMed: 33728499]

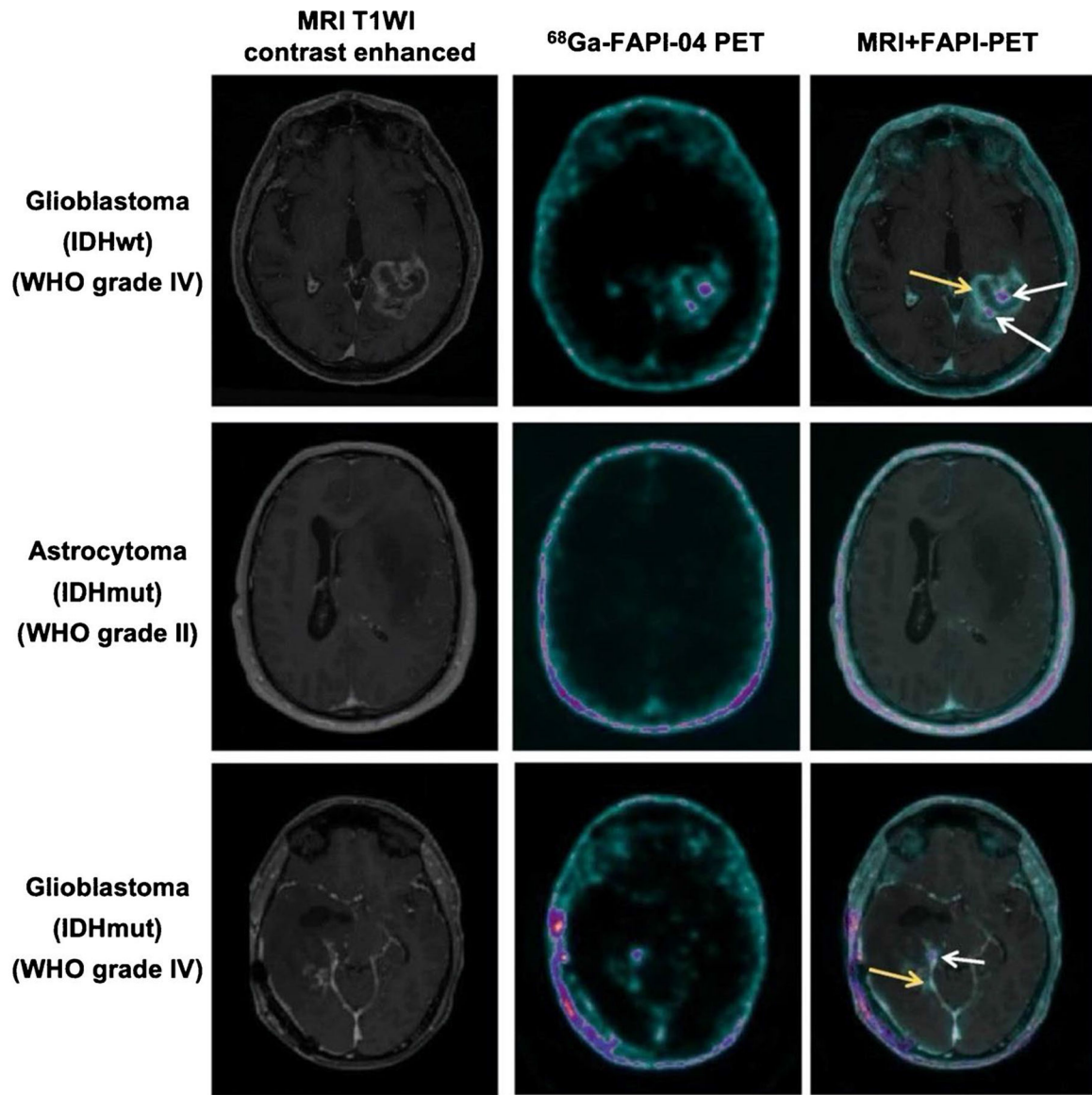
146. Hertz S, Roberts A. Radioactive iodine in the study of thyroid physiology; the use of radioactive iodine therapy in hyperthyroidism. *J Am Med Assoc.* 1946;131:81–6. 10.1001/jama.1946.02870190005002. [PubMed: 21025609]
147. Liu J, Huang C, Peng C, Xu F, Li Y, Yutaka Y, et al. Stromal fibroblast activation protein alpha promotes gastric cancer progression via epithelial-mesenchymal transition through Wnt/ $\beta$ -catenin pathway. *BMC Cancer.* 2018;18:1099. 10.1186/s12885-018-5035-9. [PubMed: 30419872]
148. Jia J, Martin TA, Ye L, Meng L, Xia N, Jiang WG, et al. Fibroblast activation protein- $\alpha$  promotes the growth and migration of lung cancer cells via the PI3K and sonic hedgehog pathways. *Int J Mol Med.* 2018;41:275–83. 10.3892/ijmm.2017.3224. [PubMed: 29115573]
149. Barreira da Silva R, Laird ME, Yatim N, Fiette L, Ingersoll MA, Albert ML. Dipeptidylpeptidase 4 inhibition enhances lymphocyte trafficking, improving both naturally occurring tumor immunity and immunotherapy. *Nat Immunol.* 2015; 16: 850–8. 10.1038/ni.3201. [PubMed: 26075911]
150. Okondo MC, Johnson DC, Sridharan R, Go EB, Chui AJ, Wang MS, et al. DPP8 and DPP9 inhibition induces procaspase-1-dependent monocyte and macrophage pyroptosis. *Nat Chem Biol.* 2017;13:46–53. 10.1038/nchembio.2229. [PubMed: 27820798]
151. Henry LR, Lee HO, Lee JS, Klein-Szanto A, Watts P, Ross EA, et al. Clinical implications of fibroblast activation protein in patients with colon cancer. *Clin Cancer Res.* 2007;13:1736–41. 10.1158/1078-0432.CCR-06-1746. [PubMed: 17363526]
152. Sollini M, Kirienko M, Gelardi F, Fiz F, Gozzi N, Chiti A. 2021 State-of-the-art of FAPI-PET imaging: a systematic review and meta-analysis. *Eur J Nucl Med Mol Imaging.* 10.1007/s00259-021-05475-0
153. Treglia G, Muoio B, Roustaei H, Kiamanesh Z, Aryana K, Sadeghi R. Head-to-head comparison of fibroblast activation protein inhibitors (FAPI) radiotracers versus [(18)F]F-FDG in oncology: a systematic review. *Int J Mol Sci.* 2021;22. 10.3390/ijms222011192.
154. Chen H, Pang Y, Wu J, Zhao L, Hao B, Wu J, et al. Comparison of [(68)Ga]Ga-DOTA-FAPI-04 and [(18)F] FDG PET/CT for the diagnosis of primary and metastatic lesions in patients with various types of cancer. *Eur J Nucl Med Mol Imaging.* 2020;47:1820–32. 10.1007/s00259-020-04769-z. [PubMed: 32222810]
155. Chen H, Zhao L, Ruan D, Pang Y, Hao B, Dai Y, et al. Usefulness of [(68)Ga]Ga-DOTA-FAPI-04 PET/CT in patients presenting with inconclusive [(18)F]FDG PET/CT findings. *Eur J Nucl Med Mol Imaging.* 2021;48:73–86. 10.1007/s00259-020-04940-6. [PubMed: 32588089]
156. Mona CE, Benz MR, Hikmat F, Grogan TR, Luckerath K, Razmaria A, et al. 2021 Correlation of (68)Ga-FAPi-46 PET biodistribution with FAP expression by immunohistochemistry in patients with solid cancers: a prospective translational exploratory study. *J Nucl Med.* 10.2967/jnumed.121.262426
157. Gundogan C, Komek H, Can C, Yildirim OA, Kaplan I, Erdur E, et al. Comparison of 18F-FDG PET/CT and 68Ga-FAPI-04 PET/CT in the staging and restaging of gastric adenocarcinoma. *Nucl Med Commun.* 2021. 10.1097/MNM.0000000000001489.
158. Lan L, Liu H, Wang Y, Deng J, Peng D, Feng Y, et al. 2021 The potential utility of [(68)Ga]Ga-DOTA-FAPI-04 as a novel broad-spectrum oncological and non-oncological imaging agent-comparison with [(18)F]FDG. *Eur J Nucl Med Mol Imaging.* 10.1007/s00259-021-05522-w
159. Liu H, Liu L, Chen L, Zhao Y, Zhang W, Cai L, et al. [(68)Ga]Ga-DOTA-FAPI-04 PET/CT imaging of benign pulmonary solitary fibrous tumour. *Eur J Nucl Med Mol Imaging.* 2021;48:2053–4. 10.1007/s00259-021-05199-1. [PubMed: 33462631]
160. Wang R, Liu Q, Sui H, Zhang M, Zhu Z, Cui R. (68)Ga-FAPI outperforms (18)F-FDG PET/CT in identifying solitary fibrous tumor. *Eur J Nucl Med Mol Imaging.* 2021;48:2055–6. 10.1007/s00259-020-05181-3. [PubMed: 33469685]
161. Zhang A, Zhang H, Zhou X, Li Z, Li N. Solitary fibrous tumors of the pleura shown on 18F-FDG and 68Ga-DOTA-FAPI-04 PET/CT. *Clin Nucl Med.* 2021;46:e534–7. 10.1097/RLU.0000000000003598. [PubMed: 33826564]
162. Chen H, Pang Y, Meng T, Yu X, Sun L. 18F-FDG and 68Ga-FAPI PET/CT in the evaluation of ground-glass opacity nodule. *Clin Nucl Med.* 2021;46:424–6. 10.1097/RLU.0000000000003600. [PubMed: 33782300]

163. Zhao L Pang Y Sun L Lin Q Chen H 2021 Increased 68Ga-FAPI uptake in the pulmonary cryptococcus and the postradiotherapy inflammation ClinNucl Med 10.1097/RLU.0000000000003873
164. Zhu W, Guo F, Wang Y, Ding H, Huo L. 68Ga-FAPI-04 accumulation in myocardial infarction in a patient with neuroendocrine carcinoma. Clin Nucl Med. 2020;45:1020–2. 10.1097/RLU.0000000000003334. [PubMed: 33086274]
165. Chandra P, Nath S, Krishnamoorthy J, Sogunuru GP. Incidental detection of ischemic myocardium on (68) Ga-FAPI PET/CT. Nucl Med Mol Imaging. 2021;55:194–8. 10.1007/s13139-021-00704-8. [PubMed: 34422130]
166. Qin C, Gai Y, Liu Q, Shao F, Lan X. Elevated 68Ga-FAPI accumulation in a recurrent angiomyolipoma. Clin Nucl Med. 2020;45:1034–5. 10.1097/RLU.0000000000003345. [PubMed: 33086278]
167. Xing HQ Gong JN Chen BX Guo XJ Yang YH Huo L et al. 2021 Comparison of (68)Ga-FAPI imaging and cardiac magnetic resonance in detection of myocardial fibrosis in a patient with chronic thromboembolic pulmonary hypertension J NuclCardiol 10.1007/s12350-020-02517-2
168. Yang X You Z Mou C Hu Z Liu H 2021 Esophagitis mimicking esophageal cancer on 68Ga-FAPI PET/CT ClinNucl Med 10.1097/RLU.0000000000003907
169. Yang X Huang Y Mou C Liu H Chen Y 2021 Chronic colitis mimicking malignancy on 68Ga-FAPI PET/CT ClinNucl Med 10.1097/RLU.0000000000003793
170. Xu T Zhao Y Ding H Cai L Zhou Z Song Z et al. 2020 [(68)Ga] Ga-DOTA-FAPI-04 PET/CT imaging in a case of prostate cancer with shoulder arthritis Eur J Nucl Med Mol Imaging 10.1007/s00259-020-05028-x
171. Luo Y, Pan Q, Yang H, Li F, Zhang F. Inflammatory arthritis induced by anti-programmed death-1 shown in 68Ga-FAPI PET/CT in a patient with esophageal carcinoma. Clin Nucl Med. 2021;46:431–2. 10.1097/RLU.0000000000003608. [PubMed: 33782307]
172. Wu J Qiu L Wang Y Zhang C 2021 Dermatomyositis on 68Ga-FAPI PET/CT in a patient with nasopharyngeal carcinoma ClinNucl Med 10.1097/RLU.0000000000003809
173. Zheng J, Chen H, Lin K, Yao S, Miao W. [(68)Ga]Ga-FAPI and [(18)F]FDG PET/CT images in a patient with juvenile polymyositis. Eur J Nucl Med Mol Imaging. 2021;48:2051–2. 10.1007/s00259-020-05185-z. [PubMed: 33462628]
174. Xu T Huang Y Zhao Y Wang P Chen Y 2021 68Ga-DOTA-FAPI-04 PET/CT Imaging in a case of SAPHO syndrome ClinNucl Med 10.1097/RLU.0000000000003901
175. Zhou Y, He J, Chen Y. (68)Ga-FAPI PET/CT imaging in a patient with thyroiditis. Endocrine. 2021;73:485–6. 10.1007/s12020-021-02605-4. [PubMed: 33449295]
176. Can C, Gundogan C, Guzel Y, Kaplan I, Komek H. 68Ga-FAPI uptake of thyroiditis in a patient with breast cancer. Clin Nucl Med. 2021;46:683–5. 10.1097/RLU.0000000000003637. [PubMed: 33826569]
177. Hotta M, Sonni I, Benz MR, Gafita A, Bahri S, Shuch BM, et al. (68)Ga-FAPI-46 and (18)F-FDG PET/CT in a patient with immune-related thyroiditis induced by immune checkpoint inhibitors. Eur J Nucl Med Mol Imaging. 2021;48:3736–7. 10.1007/s00259-021-05373-5. [PubMed: 33914106]
178. Sonni I Lee-Felker S Memarzadeh S Quinn MM Mona CE Luckerath K et al. 2020 (68)Ga-FAPi-46 diffuse bilateral breast uptake in a patient with cervical cancer after hormonal stimulation Eur J Nucl Med Mol Imaging 10.1007/s00259-020-04947-z
179. Wang LJ, Zhang Y, Wu HB. Intense diffuse uptake of 68Ga-FAPI-04 in the breasts found by PET/CT in a patient with advanced nasopharyngeal carcinoma. Clin Nucl Med. 2021;46:e293–5. 10.1097/RLU.0000000000003487. [PubMed: 33351506]
180. Zheng J, Lin K, Zheng S, Yao S, Miao W. 68Ga-FAPI and 18F-PET/CT images in intestinal tuberculosis. Clin Nucl Med. 2021. 10.1097/RLU.0000000000003917.
181. Pan Q, Luo Y, Zhang W. Idiopathic retroperitoneal fibrosis with intense uptake of 68Ga-fibroblast activation protein inhibitor and 18F-FDG. Clin Nucl Med. 2021;46:175–6. 10.1097/RLU.0000000000003402. [PubMed: 33208623]
182. Hayrapetian A, Girgis MD, Yanagawa J, French SW, Schelbert HR, Auerbach MS, et al. Incidental detection of elastofibroma dorsi with 68Ga-FAPI-46 and 18F-FDG

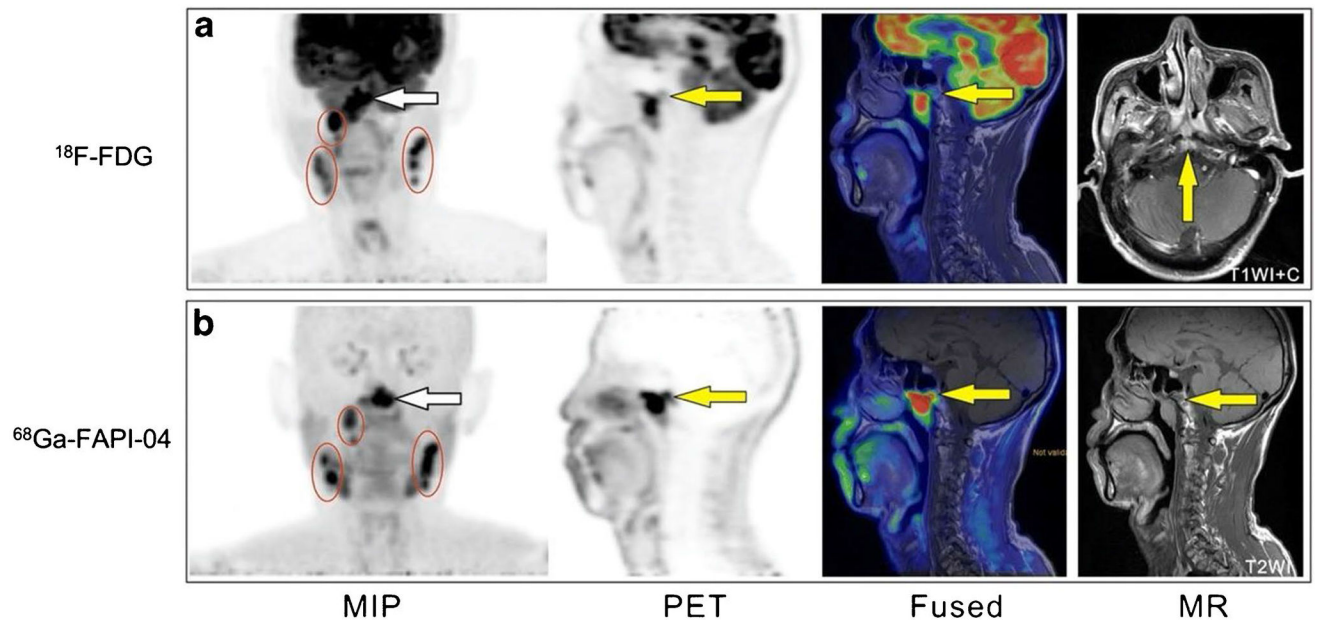
- PET/CT in a patient with esophageal cancer. *Clin Nucl Med.* 2021;46:e86–7. 10.1097/RLU.0000000000003218. [PubMed: 32701818]
183. Jiang C, Song S. 68Ga-FAPI and 18F-FDG PET/CT in perineum extramammary paget disease. *Clin Nucl Med.* 2021;46:342–4. 10.1097/RLU.0000000000003523. [PubMed: 33577199]
184. Liu H, Yang X, Wang Y, Wang P, Chen Y. 68Ga-FAPI PET/CT imaging of graves ophthalmopathy in a patient with esophageal cancer. *Clin Nucl Med.* 2021;46:938–9. 10.1097/RLU.0000000000003703. [PubMed: 34028423]
185. Zhu Y Wu J Wang Y Geng J Zhang C 2021 Presacral benign schwannoma mimics malignancy on 18F-FDG and 68Ga-FAPI PET/CT *ClinNucl Med* 10.1097/RLU.0000000000003933







**Fig. 2.** Axial view images (contrast-enhanced T1-weighted MRI, <sup>68</sup> Ga-FAPI-04 PET and fused images of both modalities) of an IDH-wildtype glioblastoma, an IDH-mutant astrocytoma, and an IDH-mutant glioblastoma. The IDH-wildtype glioblastoma and the high-grade IDH-mutant glioblastoma both show foci with moderately to markedly increased tracer uptake (white arrows and yellow arrows) within the contrast-enhancing lesion. In contrast, the tracer uptake showed only slightly elevated in IDH-mutant astrocytoma and very low in healthy brain parenchyma. Figure adapted from Rohrich et al. [46]

**Fig. 3.**

A 58-year-old man with nonkeratinizing undifferentiated carcinoma of the nasopharynx.  $^{18}\text{F}$ -FDG PET/MR (a) and  $^{68}\text{Ga}$ -FAPI-04 PET/MR (b) both demonstrate intense tracer uptake at the NPC primary site (white arrow) and at multiple lymph nodes (circles) on both sides of the neck.  $^{68}\text{Ga}$ -FAPI-04 PET/MR revealed the involvement of the occipital slope (yellow arrow) more clearly than  $^{18}\text{F}$ -FDG. Figure adapted from Qin et al. [39]

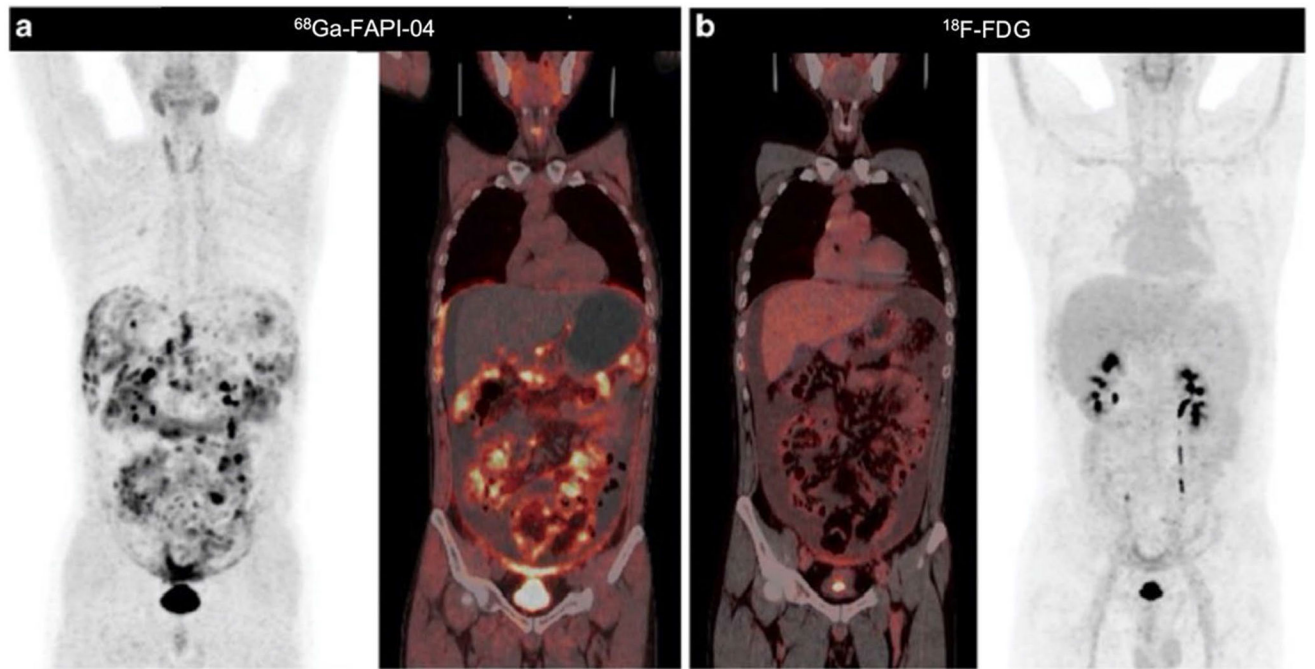


**Fig. 4.**

A 44-year-old man with a history of gastrectomy for gastric signet ring cell carcinoma presented with symptoms of abdominal pain and rising carcinoembryonic antigen levels. He underwent a PET/CT scan to detect recurrence.  $^{68}\text{Ga-FAPI-04}$  PET/CT images show intense activity throughout the abdomen and pelvis, especially around the liver and small bowel mesenterium (a). However,  $^{18}\text{F-FDG}$  PET/CT images revealed much lower tracer uptake in these regions (b). Figure adapted from Zhao et al. [56]

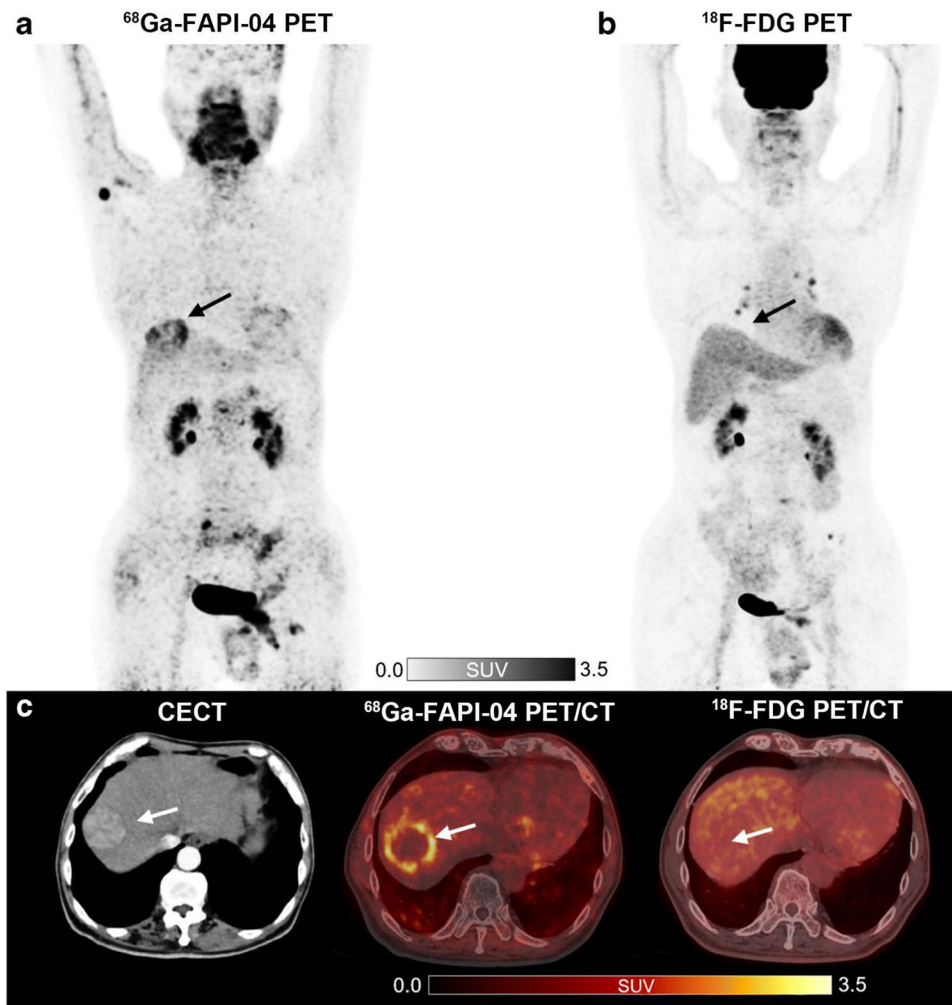


**Fig. 5.** A 78-year-old man with moderately differentiated hepatocellular carcinoma (HCC) and liver cirrhosis.  $^{68}\text{Ga-FAPI-04 PET/CT}$  (a, c) demonstrates an increased focal uptake ( $\text{SUV}_{\text{max}} = 4.05$  and  $\text{TBR} = 3.93$ ) in the liver, while  $^{18}\text{F-FDG PET/CT}$  (b, c) scans showed non-FDG-avid lesion ( $\text{SUV}_{\text{max}} = 2.55$  and  $\text{TBR} = 1.20$ ) indicated by arrows. Figure adapted from Guo et al. [64]



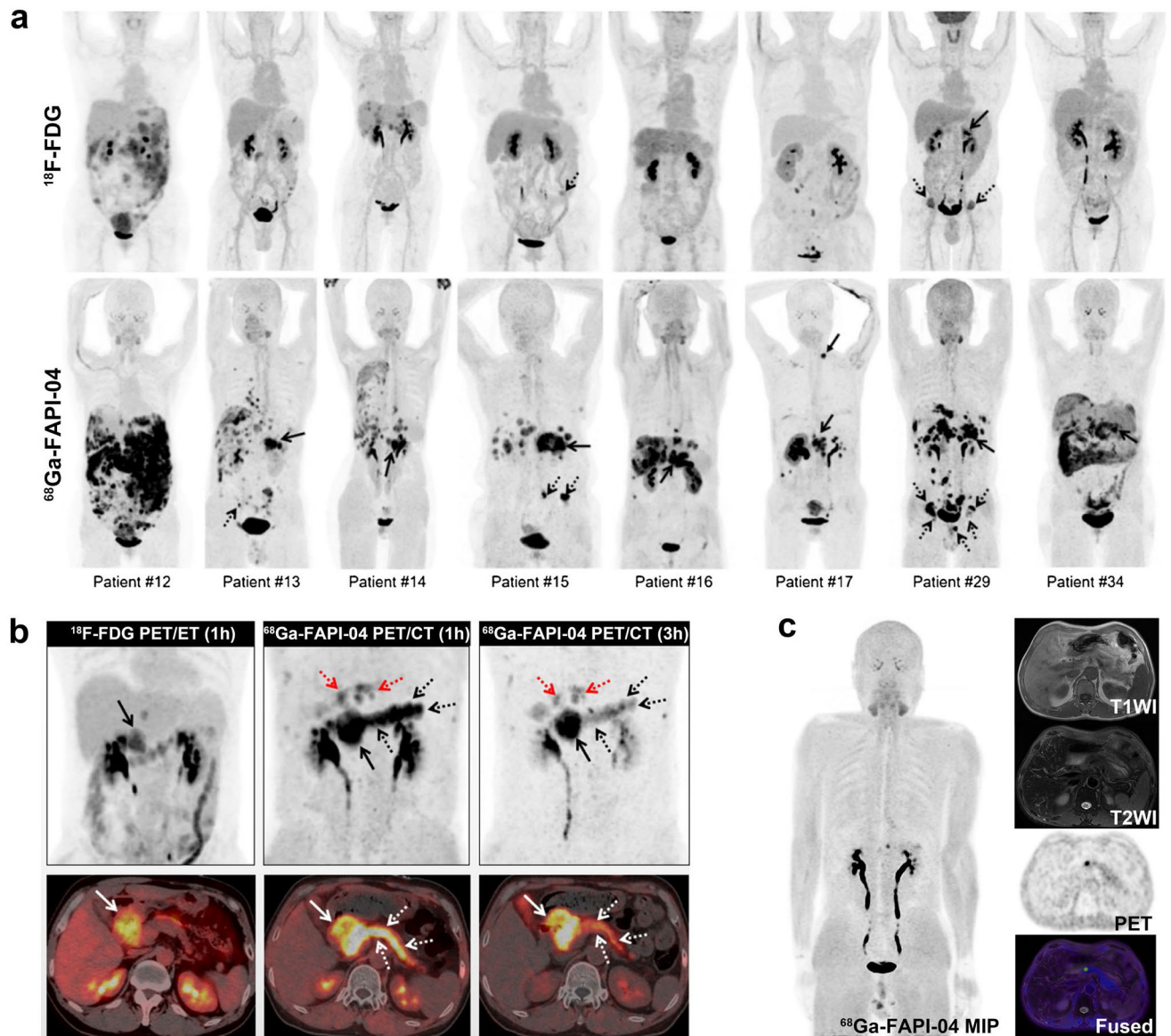


**Fig. 6.** Eight patients with pancreatic cancer underwent  $^{18}\text{F}$ -FDG and  $^{68}\text{Ga}$ -FAPI-04 PET/CT imaging.  $^{68}\text{Ga}$ -FAPI-04 PET/CT outperformed  $^{18}\text{F}$ -FDG in detecting primary tumors (solid arrows), supraclavicular lymph node metastases (arrowhead), abdomen lymph node metastases, liver metastases, peritoneal carcinomatosis, and bone metastases (dotted arrows) (a). The patient with pancreatic cancer was visible the high metabolic activity of the primary tumor on the  $^{18}\text{F}$ -FDG PET/CT and  $^{68}\text{Ga}$ -FAPI-04 PET/CT scan (solid arrows). However, the 1-h image for  $^{68}\text{Ga}$ -FAPI-04 PET/CT (middle line) demonstrated intense  $^{68}\text{Ga}$ -FAPI-04 uptake in the body and tail of the pancreas (white and black dotted arrows) and moderate FAPI uptake in the intrahepatic bile duct (red dotted arrows). 3-h delayed  $^{68}\text{Ga}$ -FAPI-04 PET was performed to differentiate between malignant and benign lesions (right line). The SUVmax value of the primary tumor was slightly elevated, whereas the SUVmax values of the pancreatitis lesions were decreased compared to the 1-h standard image (b). A 53-



year-old man suffered from retrosternal and laryngeal discomfort for more than 9 months. Laboratory testing revealed a high CEA level (11.3  $\mu\text{g/L}$ ).  $^{68}\text{Ga}$ -FAPI-04 PET/MR revealed focal uptake in the pancreatic neck with a negative corresponding MR signal. Furthermore, no abnormal lesions were found in subsequent DCE-MRI and EUS (c). Figure adapted from Pang et al. [71] and Zhang et al. [72]

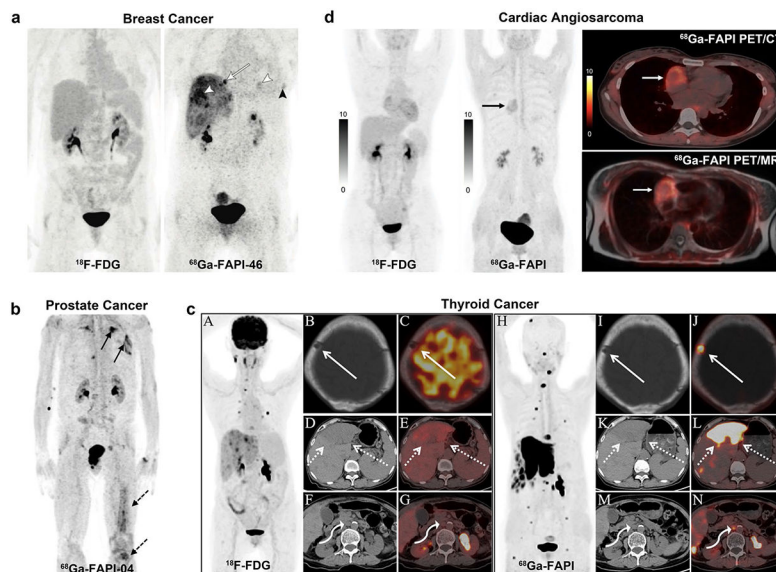


**Fig. 7.**

(a) A 60-year-old woman with triple-negative breast cancer. Neither liver and lung metastases (morphologically observed) nor local relapse demonstrated pathologic uptake in  $^{18}\text{F}$ -FDG PET. However,  $^{68}\text{Ga}$ -FAP1-46 PET showed elevated tracer uptake in metastatic lesions (white arrowheads) and local relapse (black arrowhead). Additional osseous metastasis that was previously not discernible is noted (arrow). (b) A 70-year-old patient was diagnosed with CRPC.  $^{68}\text{Ga}$ -FAP1-04 PET/CT demonstrated bone (dotted arrows) and pulmonary metastases (solid arrows). (c) A 76-year-old woman previously underwent total thyroidectomy surgery to treat papillary thyroid carcinoma. The  $^{68}\text{Ga}$ -FAP1 PET/CT showed more and higher metabolic lesions than  $^{18}\text{F}$ -FDG (it was unclear which specific FAPI-based tracer was used in this study, likely  $^{68}\text{Ga}$ -FAP1-04).  $^{18}\text{F}$ -FDG PET/CT showed destruction of the skull without  $^{18}\text{F}$ -FDG uptake (solid arrow), liver mass with moderate FDG uptake (dotted arrows), and enlarged retroperitoneal lymph node with mild FDG uptake (curved arrow). The axial of  $^{68}\text{Ga}$ -FAP1 PET/CT showed destruction of the skull with intensive FAPI uptake, liver mass with intensive FAPI uptake, and enlarged retroperitoneal lymph node with moderate FAPI uptake. (d) A 31-year-old woman presented with a history of chest pain. Ultrasonography showed massive pericardial effusion, and subsequent pericardiocentesis drained the bloody pericardial effusion. The patient underwent  $^{18}\text{F}$ -FDG to detect the primary tumor; however, no abnormal activity was observed. Follow-up with  $^{68}\text{Ga}$ -FAP1 PET/CT was performed to improve detection (it was unclear which specific FAPI-based tracer was used in this study, likely  $^{68}\text{Ga}$ -FAP1-04). A focus with increased  $^{68}\text{Ga}$ -FAP1 uptake in the right chest was revealed (black arrow). The axial PET/CT views localized this abnormality in the right atrium (white arrow), with a target/myocardium ratio of 3.9. Figure adapted from Backhaus et al. [76], Kesch et al. [86], Wu et al. [91] and Zhao et al. [94]

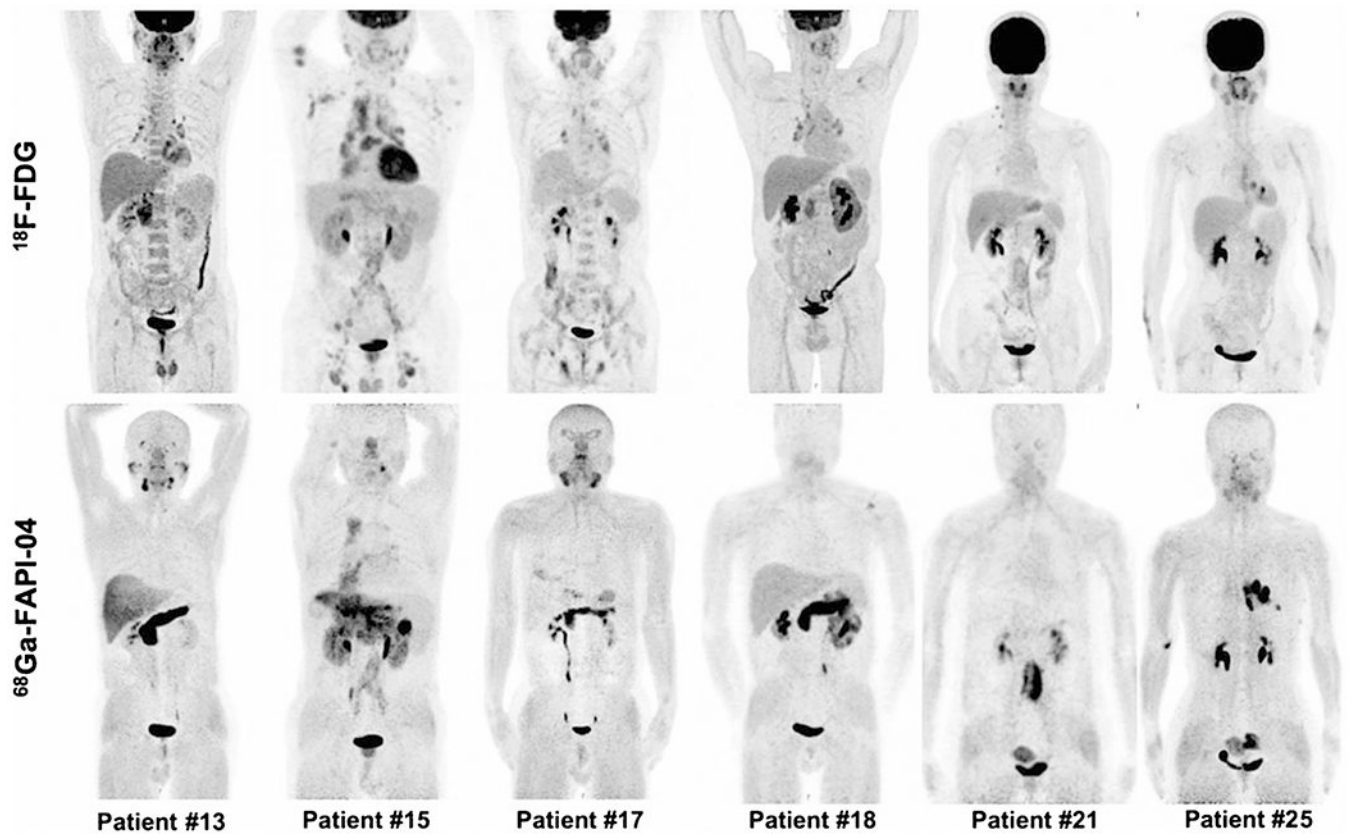


**Fig. 8.** Intraindividual comparison of 6 patients with IgG4-RD undergoing  $^{18}\text{F}$ -FDG and  $^{68}\text{Ga}$ -FAPI-04 PET/CT. Examples show superiority of  $^{68}\text{Ga}$ -FAPI-04 to  $^{18}\text{F}$ -FDG in depicting involvement of IgG4-RD in the pancreas (patients 13, 15, 17, and 18), bile duct/liver (patients 13, 15, and 17), retroperitoneal fibrosis (patient 21), lung/pleura (patient 25), and salivary gland (patients 13 and 17). Hypermetabolic lymph nodes in  $^{18}\text{F}$ -FDG-PET/CT did not show uptake of  $^{68}\text{Ga}$ -FAPI-04 (patients 15 and 17). Renal involvement (patients 15 and 18) was both  $^{18}\text{F}$ -FDG-avid and  $^{68}\text{Ga}$ -FAPI-04-avid. There was also unspecific  $^{68}\text{Ga}$ -FAPI-04 uptake in the uterus (patients 21 and 25). Figure adapted from Luo et al. [97]

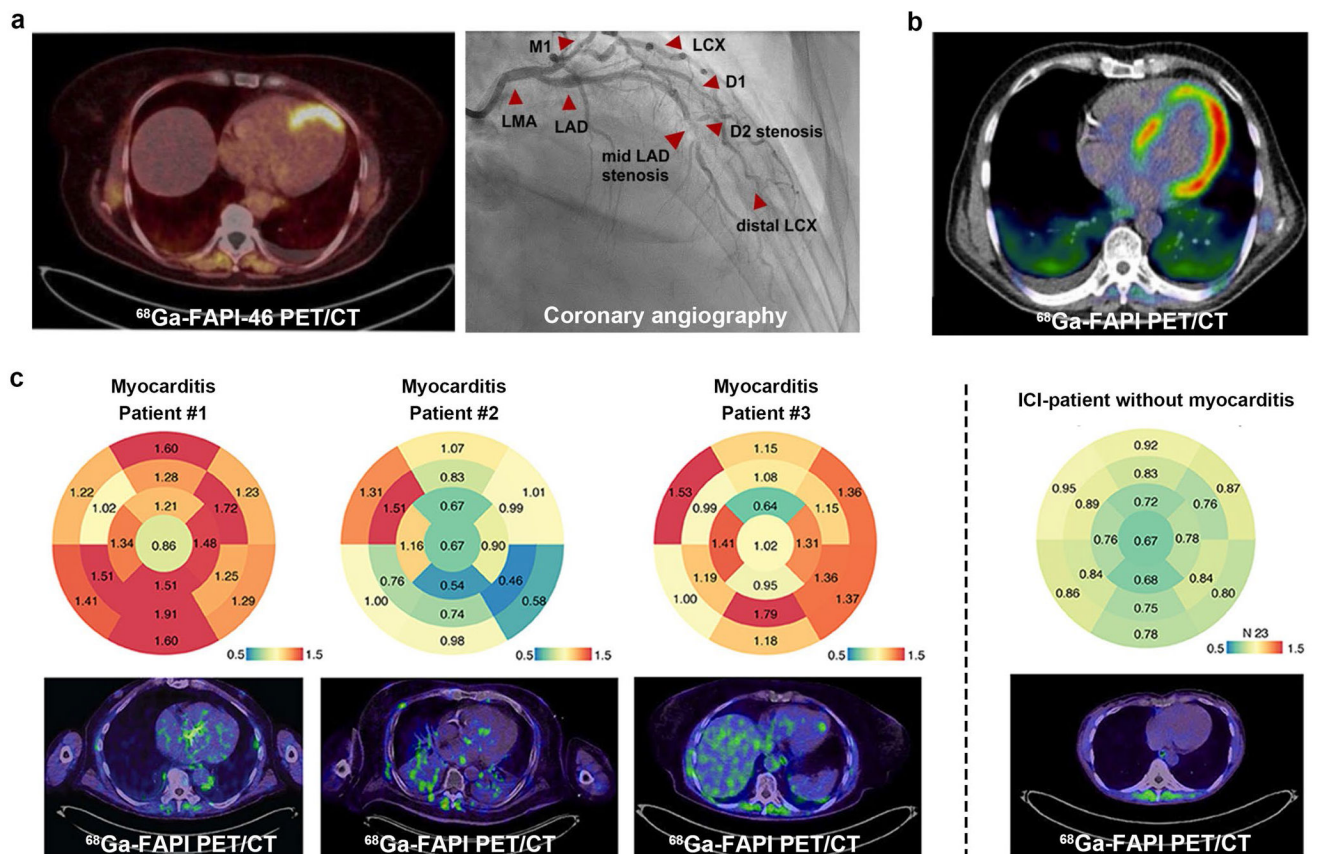


**Fig. 9.** Representative  $^{68}\text{Ga}$ -FAPI PET images of cardiovascular disease. **(a)** A 62-year-old woman presenting with STEMI underwent FAPI PET imaging 9 days after angiography. The subtotal stenosis of the mid-LAD is visualized perfectly matching the apical/apicoseptal tracer uptake in the PET scan. **(b)** A 67-year-old male patient with pancreatic ductal adenocarcinoma had received systemic cancer therapy with gemcitabine and Nab-Paclitaxel. During the disease,  $^{68}\text{Ga}$ -FAPI PET showed an intensive tracer accumulation of the left ventricular myocardium, indicating it may be capable of detecting chemotherapy-induced myocardial injuries (it was unclear which specific FAPI-based tracer was used in this study, likely  $^{68}\text{Ga}$ -FAPI-04). **(c)**  $^{68}\text{Ga}$ -FAPI PET/CT illustrates ICI-associated myocarditis. Bulls Eye Illustration of SUVs showing their distribution in the myocardium of the left ventricle in 17 defined areas. The enrichment is shown for ICI-associated myocarditis patients #1-#3 (left panel). In comparison, the median signal of patients who have received immune checkpoint inhibitors without signs of myocarditis is summarized (right panel). STEMI, ST-segment elevation myocardial infarction; LAD, left anterior descending (artery); D1, D2, diagonal branches of LAD. Figure adapted from Kessler et al. [103], Totzeck et al. [110] and Finke et al. [113]

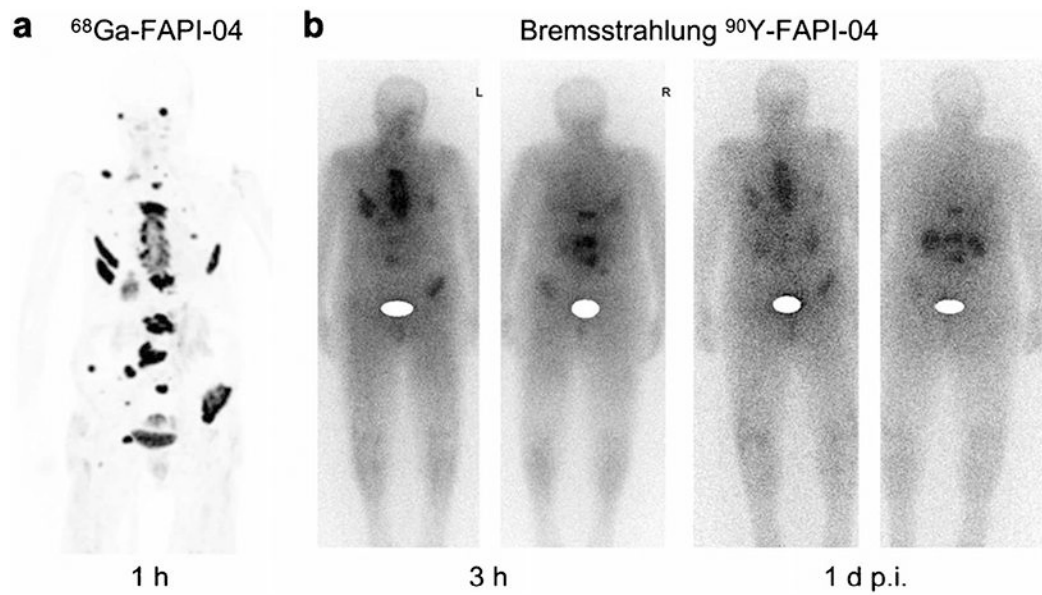


**Fig. 10.** PET maximum-intensity projection of a patient with metastasized breast cancer 1 h after administration of 270 MBq of  $^{68}\text{Ga}$ -FAPI-04. Robust uptake is seen in metastases (a). Bremsstrahlung images showing uptake at 3 h and even 1 day after treatment with  $^{90}\text{Y}$ -FAPI-04 in same patient (b). Figure adapted from Lindner et al. [35]



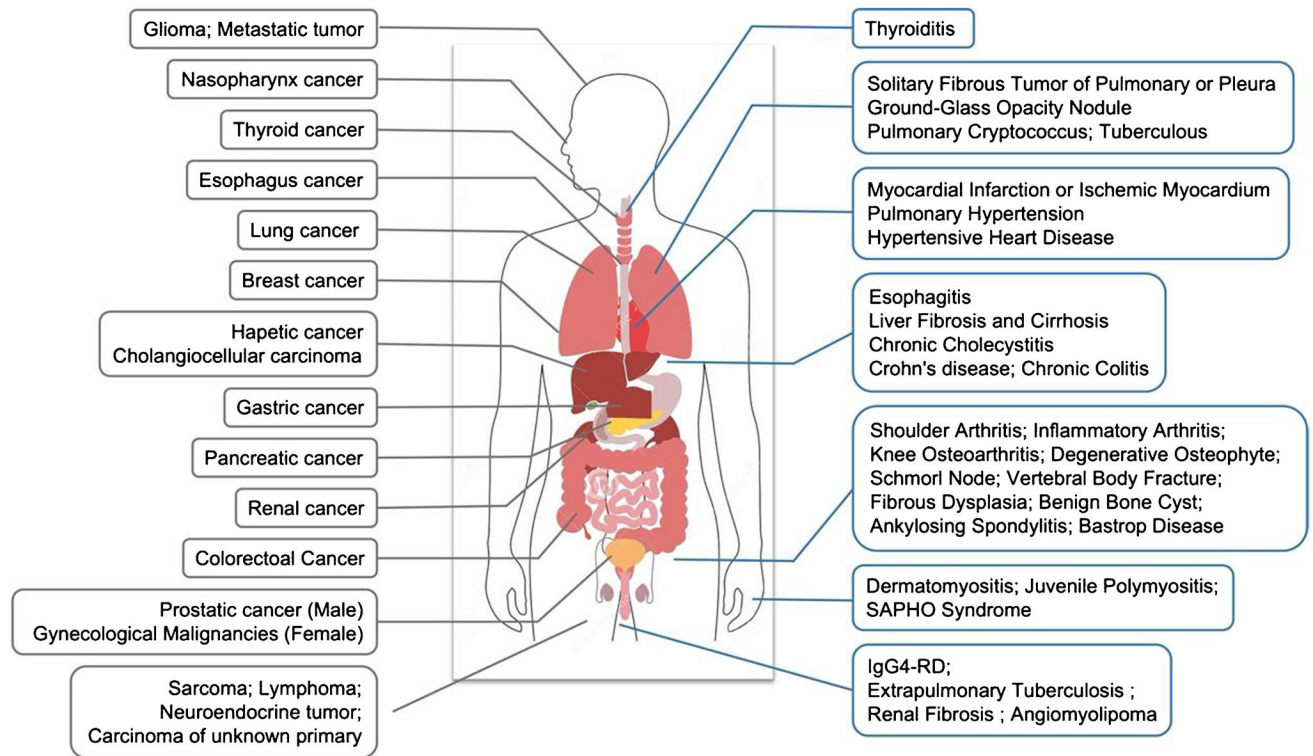


**Fig. 11.**  
 A summary of FAPI-based PET/SPECT imaging in human oncological (left side) and non-oncological (right side) diseases



Table 1

Summary of representative clinical studies evaluating FAPI PET/CT

Authors	Year	Radiopharmaceutical	Population	Number of patients	Method	Ref
Lindner et al	2018	<sup>68</sup> Ga-FAPI-04	Breast cancer	2	Prospective	[35]
Giesel et al	2019	<sup>68</sup> Ga-FAPI-02/04; <sup>18</sup> F-FDG	Mixed population of different cancers	50	Prospective	[27]
Hathl et al	2019	<sup>68</sup> Ga-FAPI-04	Mixed population of different cancers	54	Prospective	[33]
Röhrich et al	2019	<sup>68</sup> Ga-FAPI-02/04	Glioma	18	Prospective	[46]
Chen et al	2020	<sup>68</sup> Ga-FAPI-04; <sup>18</sup> F-FDG	Mixed population of different cancers	75	Prospective	[154]
Chen et al	2020	<sup>68</sup> Ga-FAPI-04; <sup>18</sup> F-FDG	Mixed patients with inconclusive <sup>18</sup> F-FDG findings	68	Prospective	[155]
Syed et al	2020	<sup>68</sup> Ga-FAPI-04	Head and neck cancers	14	Prospective	[134]
Giesel et al	2020	<sup>18</sup> F-FAPI-74; <sup>68</sup> Ga-FAPI-74	Lung cancers	10	Prospective	[42]
Shi et al	2020	<sup>68</sup> Ga-FAPI-04	Hepatobiliary cancers	25	Prospective	[66]
Koerber et al	2020	<sup>68</sup> Ga-FAPI-04/46	Colorectal and anal cancers	16	Prospective	[60]
Luo et al	2020	<sup>68</sup> Ga-FAPI-04; <sup>18</sup> F-FDG	IgG4-RD	26	Prospective	[97]
Lindner et al	2020	<sup>99m</sup> Tc-FAPI-34	Ovarian and pancreatic cancers	2	Prospective	[144]
Zhang et al	2021	<sup>68</sup> Ga-FAPI-04	Mixed patients with different diseases	103	Retrospective	[72]
Zhao et al	2021	<sup>68</sup> Ga-DOTA-2P(FAPI) <sub>2</sub>	Healthy volunteers and different cancer patients	6	Prospective	[141]
Mona et al	2021	<sup>68</sup> Ga-FAPI-46	Mixed patients with different diseases	141	Prospective	[156]
Gundogan et al	2021	<sup>68</sup> Ga-FAPI-04	Gastric adenocarcinoma	21	Prospective	[157]
Pang et al	2021	<sup>68</sup> Ga-FAPI-04	Pancreatic cancers	36	Retrospective	[71]
Ballal et al	2021	<sup>68</sup> Ga-DOTA.SA.FAPI	Radioiodine-refractory differentiated thyroid cancer	15	Prospective	[143]
Lan et al	2021	<sup>68</sup> Ga-FAPI-04	Mixed patients with different diseases	123	Prospective	[158]
Kuten et al	2021	<sup>68</sup> Ga-FAPI-04	Gastric adenocarcinoma	13	Prospective	[57]
Qin et al	2021	<sup>68</sup> Ga-FAPI-04	Nasopharyngeal carcinoma	15	Prospective	[39]
Qin et al	2021	<sup>68</sup> Ga-FAPI-04	Gastric carcinomas	20	Prospective	[59]

Table 2

Case-based reports of  $^{68}\text{Ga}$ -FAPI variants imaging in non-cancerous patients

Tissue/organ	Diseases	Ref	
Respiratory system	Solitary fibrous tumor of pulmonary or pleura	[159–161]	
	Ground-glass opacity nodule	[162]	
	Pulmonary cryptococcus	[163]	
Cardiovascular system	Myocardial infarction; ischemic myocardium	[103, 164, 165]	
	Angiomyolipoma	[166]	
	Chronic thromboembolic pulmonary hypertension	[107, 167]	
Digestive system	Hypertensive heart disease	[109]	
	Esophagitis	[168]	
	Crohn's disease; chronic colitis	[131, 169]	
	Chronic cholecystitis	[116]	
	Shoulder arthritis;	[170]	
Musculoskeletal system	Inflammatory arthritis	[171]	
	Knee osteoarthritis	[126]	
	Degenerative osteophyte	[116, 117]	
	Schmorl node	[118]	
	Vertebral body fracture	[119, 120]	
	Fibrous dysplasia	[122, 123]	
	Benign bone cyst	[121]	
	Ankylosing spondylitis	[124]	
	Baastrop disease	[125]	
	Dermatomyositis; juvenile polymyositis	[172, 173]	
	SAPHO syndrome	[174]	
	Gland	Thyroiditis	[175–177]
		Breasts	[178, 179]
Other	IgG4-RD	[98–100]	
	Tuberculous lesions; extrapulmonary Tuberculosis	[128, 129, 180]	
	Renal fibrosis	[133]	
	Idiopathic retroperitoneal fibrosis	[181]	

Tissue/organ	Diseases	Ref
	Elastofibroma dorsi	[182]
	Erdheim-Chester disease	[130]
	Perineum Paget disease	[183]
	Graves ophthalmopathy	[184]
	Presacral benign schwannoma	[185]
	Benign lymphoid tissue in cancer patient	[81]

*SAPHO* syndrome: synovitis, acne, pustulosis, hyperostosis, and osteitis syndrome; *IgG4-RD*, immunoglobulin G4-related disease